reported to be conserved in HTLV-1 provirus, and PCR for this region was used to measure total PVL.[23,25] Ohshima *et al.*[25] reported that variation of DNA sequence is frequently detected in the *gag* region of HTLV-1 provirus in patients with ATL. Kamihira *et al.*[24] also reported that most of deficient provirus in patients with ATL lacked part of the *gag* region in the proviral regions of HTLV-1 tested. HTLV-1 provirus with deletion of the 5′LTR, and its flanking internal sequences was also found in patients with ATL.[26] In our study, therefore, we tried to find provirus with deficiencies and/or polymorphism of DNA sequence in the asymptomatic carriers by measuring PVLs for the *gag* and 5′LTR-*gag* regions as ratios to *pX* region PVLs. As a result, median 5′LTR-*gag* PVL/*pX* PVL and *gag* PVL/*pX* PVL ratios of 161 HTLV-1 carriers with relatively high *pX* PVL (equal to or greater than one copy per 100 PBMCs) were 0.97 and 0.61, respectively. Our interpretation of this result was that many HTLV-1 infected cells in asymptomatic carriers harbor provirus with deficiency and/or polymorphism of DNA sequences for the sites of primers and/or probe for *gag* real time-PCR.

Long PCR analysis was performed on 17 carriers with low *gag* PVL/*pX* PVL ratios. Five of 17 carriers (29%) were shown to have the provirus with large deletions of internal DNA sequence including the *gag* region. The clonal expansion of HTLV-1 infected cells harboring defective provirus in these five carriers was most likely. In fact, clonal expansion of HTLV-1 infected cells in C1 was already shown in our previous study.[19] The reason for the low *gag* PVL/*pX* PVL ratios in the other 12 carriers was not clear. Contribution of the sum total of HTLV-1 infected cells with defective provirus, which did not reveal dense bands, was possible. Alternatively, polymorphism of the proviral DNA sequence for the *gag* region may have decreased the efficiency of real time-PCR for *gag* PVL. However, cloning and DNA sequencing of the sites for primers and probes for real time-PCR for *gag* PVL in these carriers did not show consistent polymorphism of the proviral DNA (data not shown). This may be because there is high diversity of proviral DNA sequence in the *gag* region of HTLV-1 and it was not possible to prepare cloning primers to work for all of them.

The other two (C20 and 21) showed low ratios not only of 5′LTR-*gag* PVL/*pX* PVL but also of *gag* PVL/*pX* PVL. Our previous study showed that they had high PVLs and clonal expansion of HTLV-1 infected cells with defective provirus.[19] We could not identify the type of defective provirus in the previous study. In our study, however, we found provirus lacking 5′LTR and its internal flanking region existed in these carriers.

In our study, the provirus with deficiency and/or polymorphism of the *gag* region was commonly found in asymptomatic HTLV-1 carriers. Few carriers had provirus lacking 5′LTR and its flanking sequence. Carriers with provirus with deficiency and/or polymorphism of the *gag* region were found frequently among asymptomatic carriers with high PVLs. These infected cells may not express certain HTLV-1 proteins. This change may make it possible for the HTLV-1 infected cells to avoid attack by cytotoxic T-lymphocytes.[33] Therefore, there is a possibility that provirus with deficiency and/or polymorphism of HTLV-1 provirus contributes to the survival of HTLV-1 infected cells. Indeed, our previous study showed that C1, 20 and 21 had clonal expansion of HTLV-1 infected cells.[19]

Low *gag* PVL/*pX* PVL ratio was found to be associated with maternal infection. The reason carriers with maternal infection have a greater number of HTLV-1 infected cells harboring provirus with deficiency and/or polymorphism of the *gag* region was not clear in our study. The replication of HTLV-1 infected cells in long-term infected carriers may account for this. Alternatively, a low level of new cell to cell infection *in vivo* can contribute to the creation of deficiency and/or polymorphism in proviral genome.

Maternal infection has been considered to be a risk factor for the development of ATL in asymptomatic carriers. However, there has been no method to identify infection route in the absence of information on family HTLV-1 status. The results of our study suggest the possibility that *gag* PVL/*pX* PVL ratio can be used as a tool to differentiate the infection routes of asymptomatic HTLV-1 carriers. Due to the fact that only a small number of HTLV-1 carriers with known infectious routes were analyzed in our study, further study with a larger number of subjects is necessary.

A major limitation of our study is that the subjects were elderly individuals, whose median age was 67 years old. The average age at onset of ATL was reported as 60 years.[34] Therefore, it is not clear whether the same result would be obtained from an analysis of younger HTLV-1 asymptomatic carriers. In addition, carriers with low *pX* PVL (less than 1 copy/100 PBMCs) were not provided for the analysis of deficiency and/or polymorphism of HTLV-1 proviral sequence because of technical limitations. Further analysis of carriers with low PVLs using improved methodology is necessary.

In conclusion, our study showed that *pX* PVL in carriers with maternal infection was significantly higher than that in carriers with spousal infection. Low *gag* PVL/*pX* PVL ratio reflecting deficiency and/or polymorphism in proviral genome was associated with high PVLs and maternal infection. These data suggest that development of ATL in carriers with maternal infection may be due in part to high PVL, which can be related to provirus with deficiency and/or polymorphism in proviral genome. In addition, *gag* PVL/*pX* PVL ratio has potential for use as a tool to differentiate infection routes of asymptomatic HTLV-1 carriers. Further study is necessary to clarify the mechanism of deficiency and/or polymorphism in HTLV-1 proviral genome and its implications in ATL development.

Acknowledgements

The authors thank Ms. Y. Kaseda and Ms. N. Kanemaru (Miyazaki University) for their technical assistance and Dr. M. Maeda (Kyoto University) for the gift of the HTLV-1 infected cell line, ED-40515(-).

References

1. Uchiyama T, Yodoi J, Sagawa K, Takatsuki K, Uchino H. Adult T-cell leukemia: clinical and hematologic features of 16 cases. *Blood* 1977;50:481–92.
2. Yoshida M, Miyoshi I, Hinuma Y. Isolation and characterization of retrovirus from cell lines of human adult T-cell leukemia and its implication in the disease. *Proc Natl Acad Sci USA* 1982;79: 2031–5.
3. Osame M, Usuku K, Izumo S, Ijichi N, Amitani H, Igata A, Matsumoto M, Tara M. HTLV-I associated myelopathy, a new clinical entity. *Lancet* 1986;1: 1031–2.
4. Gessain A, Barin F, Vernant JC, Gout O, Maurs L, Calender A, de The G. Antibodies to human T-lymphotropic virus type-I in patients with tropical spastic paraparesis. *Lancet* 1985;2: 407–10.
5. Hino S, Yamaguchi K, Katamine S, Sugiyama H, Amagasaki T, Kinoshita K, Yoshida Y, Doi H, Tsuji Y, Miyamoto T. Mother-to-child transmission of human T-cell leukemia virus type 1. *Jpn J Cancer Res (Gann)* 1985;76:474–80.
6. Kajiyama W, Kashiwagi S, Ikematsu H, Hayashi J, Nomura H, Okochi K. Intrafamilial transmission of adult T cell leukemia virus. *J Infect Dis* 1986;154: 851–7.
7. Okochi K, Sato H, Hinuma Y. A retrospective study on transmission of adult T cell leukemia virus by blood transfusion: seroconversion in recipients. *Vox Sang* 1984;46:245–53.
8. Arisawa K, Soda M, Endo S, Kurokawa K, Katamine S, Shimokawa I, Koba T, Takahashi T, Saito H, Doi H, Shirahama S. Evaluation of adult T-cell leukemia/ lymphoma incidence and its impact on non-Hodgkin lymphoma incidence in southwestern Japan. *Int J Cancer* 2000;85: 319–24.
9. Yamaguchi K, Watanabe T. Human T lymphotropic virus type-I and adult T-cell leukemia in Japan. *Int J Hematol* 2002; 76(Suppl 2):240–5.
10. Murphy EL, Hanchard B, Figueroa JP, Gibbs WN, Lofters WS, Campbell M, Goedert JJ, Blattner WA. Modelling the risk of adult T-cell leukemia/lymphoma in persons infected with human T-lymphotropic virus type I. *Int J Cancer* 1989;43:250–3.
11. Bartholomew C, Jack N, Edwards J, Charles W, Corbin D, Cleghorn FR, Blattner WA. HTLV-I serostatus of mothers of patients with adult T-cell leukemia and HTLV-I-associated myelopathy/tropical spastic paraparesis. *J Hum Virol* 1998;1: 302–5.
12. Wilks R, Hanchard B, Morgan O, Williams E, Cranston B, Smith ML, Rodgers-Johnson P, Manns A. Patterns of HTLV-I infection among family members of patients with adult T-cell leukemia/ lymphoma and HTLV-I associated myelopathy/tropical spastic paraparesis. *Int J Cancer* 1996; 65:272–3.
13. Seiki M, Eddy R, Shows TB, Yoshida M. Nonspecific integration of the HTLV provirus genome into adult T-cell leukaemia cells. *Nature* 1984; 309:640–2.
14. Wattel E, Vartanian JP, Pannetier C, Wain-Hobson S. Clonal expansion of human T-cell leukemia virus type I-infected cells in asymptomatic and symptomatic carriers without malignancy. *J Virol* 1995;69: 2863–8.
15. Etoh K, Tamiya S, Yamaguchi K, Okayama A, Tsubouchi H, Ideta T, Mueller N, Takatsuki K, Matsuoka M. Persistent clonal proliferation of human T-lymphotropic virus type I-infected cells in vivo. *Cancer Res* 1997;57:4862–7.
16. Cavrois M, Leclercq I, Gout O, Gessain A, Wain-Hobson S, Wattel E. Persistent oligoclonal expansion of human T-cell leukemia virus type 1-infected circulating cells in patients with Tropical spastic paraparesis/HTLV-1 associated myelopathy. *Oncogene* 1998;17:77–82.
17. Gillet NA, Malani N, Melamed A, Gormley N, Carter R, Bentley D, Berry C, Bushman FD, Taylor GP, Bangham CR. The host genomic environment of the provirus determines the abundance of HTLV-1-infected T cell clones. *Blood* 2011;117: 3113–22.
18. Tanaka G, Okayama A, Watanabe T, Aizawa S, Stuver S, Mueller N, Hsieh CC, Tsubouchi H. The clonal expansion of human T lymphotropic virus type 1-infected T cells: a comparison between seroconverters and long-term carriers. *J Infect Dis* 2005;191: 1140–7.
19. Takenouchi H, Umeki K, Sasaki D, Yamamoto I, Nomura H, Takajo I, Ueno S, Umekita K, Kamihira S, Morishita K, Okayama A. Defective human T-lymphotropic virus type 1 provirus in asymptomatic carriers. *Int J Cancer* 2010; 128:1335–43.
20. Okayama A, Stuver S, Matsuoka M, Ishizaki J, Tanaka G, Kubuki Y, Mueller N, Hsieh CC, Tachibana N, Tsubouchi H. Role of HTLV-1 proviral DNA load and clonality in the development of adult T-cell leukemia/lymphoma in asymptomatic carriers. *Int J Cancer* 2004; 110:621–5.
21. Iwanaga M, Watanabe T, Utsunomiya A, Okayama A, Uchimaru K, Koh KR, Ogata M, Kikuchi H, Sagara Y, Uozumi K, Mochizuki M, Tsukasaki K, et al. Human T-cell leukemia virus type I (HTLV-1) proviral load and disease progression in asymptomatic HTLV-1 carriers: a nationwide prospective study in Japan. *Blood* 2010;116:1211–9.
22. Iga M, Okayama A, Stuver S, Matsuoka M, Mueller N, Aoki M, Mitsuya H, Tachibana N, Tsubouchi H. Genetic evidence of transmission of human T cell lymphotropic virus type 1 between spouses. *J Infect Dis* 2002;185:691–5.
23. Tamiya S, Matsuoka M, Etoh K, Watanabe T, Kamihira S, Yamaguchi K, Takatsuki K. Two types of defective human T-lymphotropic virus type I provirus in adult T-cell leukemia. *Blood* 1996;88: 3065–73.
24. Kamihira S, Sugahara K, Tsuruda K, Minami S, Uemura A, Akamatsu N, Nagai H, Murata K, Hasegawa H, Hirakata Y, Takasaki Y, Tsukasaki K, et al. Proviral status of HTLV-1 integrated into the host genomic DNA of adult T-cell leukemia cells. *Clin Lab Haematol* 2005;27: 235–41.
25. Ohshima K, Kikuchi M, Masuda Y, Kobari S, Sumiyoshi Y, Eguchi F, Mohtai H, Yoshida T, Takeshita M, Kimura N. Defective provirus form of human T-cell leukemia virus type I in adult T-cell leukemia/lymphoma: clinicopathological features. *Cancer Res* 1991;51:4639–42.
26. Miyazaki M, Yasunaga J, Taniguchi Y, Tamiya S, Nakahata T, Matsuoka M. Preferential selection of human T-cell leukemia virus type 1 provirus lacking the 5' long terminal repeat during oncogenesis. *J Virol* 2007;81: 5714–23.
27. Korber B, Okayama A, Donnelly R, Tachibana N, Essex M. Polymerase chain reaction analysis of defective human T-cell leukemia virus type I proviral genomes in leukemic cells of patients with adult T-cell leukemia. *J Virol* 1991;65: 5471–6.
28. Yoshida M. Multiple viral strategies of HTLV-1 for dysregulation of cell growth control. *Annu Rev Immunol* 2001;19: 475–96.
29. Mueller N, Okayama A, Stuver S, Tachibana N. Findings from the Miyazaki

Cohort Study. *J Acquir Immune Defic Syndr Hum Retrovirol* 1996;13(Suppl 1): S2–7.
30. Seiki M, Hattori S, Hirayama Y, Yoshida M. Human adult T-cell leukemia virus: complete nucleotide sequence of the provirus genome integrated in leukemia cell DNA. *Proc Natl Acad Sci USA* 1983;80: 3618–22.
31. Kent WJ. BLAT—the BLAST-like alignment tool. *Genome Res* 2002;12: 656–64.
32. Roucoux DF, Wang B, Smith D, Nass CC, Smith J, Hutching ST, Newman B, Lee TH, Chafets DM, Murphy EL. A prospective study of sexual transmission of human T lymphotropic virus (HTLV)-I and HTLV-II. *J Infect Dis* 2005;191:1490–7.
33. Kannagi M. Immunologic control of human T-cell leukemia virus type I and adult T-cell leukemia. *Int J Hematol* 2007; 86:113–7.
34. Matsuoka M, Jeang KT. Human T-cell leukaemia virus type 1 (HTLV-1) infectivity and cellular transformation. *Nat Rev Cancer* 2007;7:270–80.

UICC
global cancer control

IJC
International Journal of Cancer

Defective human T-lymphotropic virus Type 1 provirus in asymptomatic carriers

Hiroyuki Takenouchi[1], Kazumi Umeki[1], Daisuke Sasaki[2], Ikuo Yamamoto[1], Hajime Nomura[1], Ichiro Takajo[1], Shiro Ueno[1], Kunihiko Umekita[1], Shimeru Kamihira[2], Kazuhiro Morishita[3] and Akihiko Okayama[1]

[1] Department of Rheumatology, Infectious Diseases and Laboratory Medicine, University of Miyazaki, Miyazaki, Japan
[2] Department of Laboratory Medicine, Nagasaki University School of Medicine, Nagasaki, Japan
[3] Division of Tumor Biochemistry, Department of Biochemistry, University of Miyazaki, Miyazaki, Japan

Few studies have specifically examined defective provirus in asymptomatic human T-lymphotropic virus Type 1 (HTLV-1) carriers and its relation to proviral DNA loads (PVLs). To assess the significance of defective provirus in asymptomatic carriers, we examined PVLs in peripheral blood mononuclear cells of 208 asymptomatic HTLV-1 carriers. The mean PVLs determined using primers for the *pol* region were less than that for the *pX* region in these carriers. Analysis of seven carriers with high PVLs for the *pX* region but lower PVLs for the *pol* region showed that four had single nucleotide polymorphisms of proviral genomes for the *pol* region and three had HTLV-1-infected cells with defective provirus. Three carriers with defective provirus showed high PVLs at their initial screens, and PVLs increased after a 10- to 12-year interval in two carriers. Southern blot assay showed clonal expansion of HTLV-1-infected cells, and the predominant clones changed during the observation period. These data suggest that although HTLV-1-infected cells with defective provirus may have a growth advantage, the predominant clones of HTLV-1-infected cells do not always survive for many years in asymptomatic carriers.

Human T-lymphotropic virus Type 1 (HTLV-1) is the causative agent of adult T-cell leukemia/lymphoma (ATL) and a progressive neurological disease known as HTLV-1-associated myelopathy/tropical spastic paraparesis (HAM/TSP).[1–4] When an individual is infected by HTLV-1, the virus randomly integrates into the genome of affected T-cells in the form of a provirus.[5] The majority of HTLV-1 carriers are asymptomatic, and only a fraction of the number of carriers develops ATL after a long latent period.[6,7] It is thought that HTLV-1 infection drives the proliferation of T-cells, leading to the clonal expansion of HTLV-1-infected cells.[8–11] A high level of HTLV-1-infected cells is considered a risk factor for developing ATL.[12]

The complete HTLV-1 provirus is ~9 kb and contains the coding regions for core protein (*gag*), protease (*pro*), polymerase (*pol*), envelope protein (*env*), regulatory proteins, such as Tax and Rex, and some accessory molecules between 5′ and 3′ long-terminal repeats (LTRs).[5,13] It has been reported that defective provirus was detectable in approximately half of patients with ATL.[14–18] Tamiya *et al.* reported two types of genome deletion in defective provirus.[16] One form (*i.e.*, Type 1) retains both LTRs and lacks internal sequences, such as the *gag* and *pol* regions. The other form (*i.e.*, Type 2) has only the 3′ LTR, and the 5′ LTR and its flanking internal sequences are preferentially deleted. HTLV-1-infected cells harboring Type 2 defective virus were frequently found in patients with ATL.[18] Defective provirus has also been reported to be detectable in asymptomatic HTLV-1 carriers. Morozov *et al.* reported that defective provirus, which lacked large internal sequences, was detectable in 18 of 20 HTLV-1 carriers.[19] However, it has not yet been determined whether the HTLV-1-infected cells with defective provirus are maintained for a long time in asymptomatic carriers and whether the defective provirus is associated with the development of ATL.

In our study, to clarify the significance of defective provirus in asymptomatic carriers, the peripheral mononuclear cells (PBMCs) of 208 HTLV-1 carriers were screened for the presence of defective provirus. Long polymerase chain reaction (PCR) and Southern blot analysis were performed to determine the changes in clonality of HTLV-1-infected cells

Key words: HTLV-1, asymptomatic carrier, proviral DNA loads
Abbreviations: ATL: adult T-cell leukemia/lymphoma; CTL: cytotoxic T-lymphocytes; HBZ: HTLV-1 basic leucine zipper factor; HTLV-1: human T-lymphotropic virus Type 1; LTR: long-terminal repeat; PBMCs: peripheral mononuclear cells; PCR: polymerase chain reaction; PVLs: proviral DNA loads
Grant sponsors: Ministry of Education, Science, Sports and Culture, Japan, Miyazaki Prefecture Collaboration of Regional Entities for the Advancement of Technological Excellence, JST
DOI: 10.1002/ijc.25450
History: Received 29 Jan 2010; Accepted 28 Apr 2010; Online 12 May 2010
Correspondence to: Akihiko Okayama, Department of Rheumatology, Infectious Diseases and Laboratory Medicine, Faculty of Medicine, University of Miyazaki, 5200 Kihara, Kiyotake, Miyazaki 889-1692, Japan, Tel: +81-985-85-7284, Fax: +81-985-85-4709, E-mail: okayama@med.miyazaki-u.ac.jp

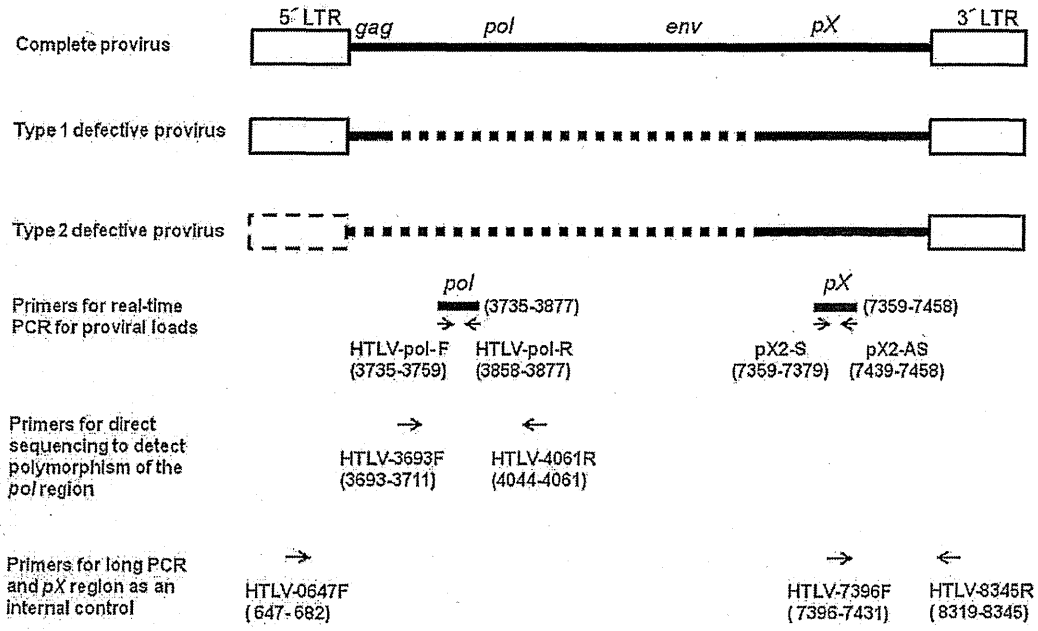

Figure 1. Schemas of structure of complete, Type 1 defective and Type 2 defective HTLV-1 (human T-lymphotropic virus Type 1) provirus. Dotted lines represent the defective regions of HTLV-1 provirus. Locations of primers for polymerase chain reactions in our study are revealed.

harboring defective provirus. Time-sequential samples of greater than 10 years obtained from asymptomatic carriers with large numbers of HTLV-1-positive cells with defective provirus were analyzed.

Material and Methods

Samples

Samples of PBMCs were obtained from 208 asymptomatic HTLV-1 carriers in the Miyazaki Cohort Study.[20] Informed consent was obtained from the study participants, and the study protocol was approved by the institutional review board at the University of Miyazaki. Genomic DNA was isolated from the PBMCs of HTLV-1 carriers by sodium dodecyl sulfate-proteinase K digestion, followed by phenol-chloroform extraction and ethanol precipitation.

Quantification of HTLV-1 provirus in PBMCs

Schemas of the structure of complete, Type 1 defective and Type 2 defective HTLV-1 provirus are shown in Figure 1.[16] The nucleotide position number of HTLV-1 provirus was according to Seiki *et al.* (accession no. J02029).[21]

Proviral DNA loads (PVLs) for the *pol* (positions 3735–3877) and *pX* (positions 7359–7458) regions were measured by real-time PCR using a Light Cycler DX 400 (Roche Diagnostics, Mannheim, Germany). When multiple time-sequential samples were available from one subject, the most recent sample was used for the first screening. The primers and the probe for the *pol* region of HTLV-1 provirus were as follows: the forward primer (HTLV-pol-F 5′-AACCAATT CATTCAAACATCTGACC-3′: positions 3735–3759), the reverse primer (HTLV-pol-R 5′-GCTTTCACAGGAGCCAA TGG-3′: positions 3877–3858) and the FAM-labeled probe (5′-FAM-TGTTCCTATCTTACTCCACCACAGTCACCGA-TA MRA-3′: positions 3767–3797).[22] The primers and the probe for the *pX* region of HTLV-1 provirus were as follows: the forward primer (pX2-S 5′-CGGATACCCAGTCTACGTGTT-3′: positions 7359–7379), the reverse primer (pX2-AS 5′-CAGTAGGG CGTGACGATGTA-3′: positions 7458–7439) and the FAM-labeled probe (5′-FAM-CTGTGTACAAGGCGACTGGTGCC-TAM RA-3′).[11] *RNase* P control Reagent (Applied Biosystems, Foster City, CA) was used for the primers and the probe for human *RNase* P DNA as internal control. PVLs were shown by the copy number of HTLV-1 provirus in 100 PBMCs.

Determination of DNA polymorphism in the *pol* primer region

To determine whether the lower PVLs for the *pol* region compared to that for the *pX* region in a same subject was due to the polymorphism of the DNA sequence of primers for the *pol* region, DNA sequence of PCR products of the *pol* region was identified in the cases described below. Primers used for PCR for this purpose were as follows: the forward primer (HTLV-3693F 5′-CTCTGCCAAACCATAC-3′: positions 3693–3711) and the reverse primer (HTLV-4061R 5′-ATGCAAAAGTCCGAGAAG-3′: positions 4061–4044). PCR products were supplied for direct sequencing using an

ABI PRISM Genetic Analyzer 310 (Applied Biosystems). To verify whether the polymorphism found affected the amplification efficiency of real-time PCR for measuring PVLs for the *pol* region, PCR products were subcloned by pGEM-T Easy vector system (Promega, Madison, WI). The amplification efficiency of real-time PCR for the *pol* region was compared between the DNA sequences with and without this polymorphism.

Detection of Type 1 defective provirus by long PCR

To assess whether the Type 1 defective provirus exists in the HTLV-1 carriers with lower PVLs for the *pol* region compared to those for the *pX* region, long PCR, which amplifies the complete provirus and the Type 1 defective provirus with 5′ LTR conserved, was performed. The primers were as follows: 5′LTR(HTLV-0647F 5′-GTTCCACCCCTTTCCCTTTC ATTCACGACTGACTGC-3′: positions 647–682) and 3′LTR (HTLV-8345R 5′-GGCTCTAAGCCCCCGGGGGATATTTG GGGCTCATGG-3′: positions 8345–8319).[18] Long PCR was performed using LA Taq DNA polymerase (Takara Bio, Shiga, Japan). Cycles for long PCR were as follows: one cycle of 98°C for 20 sec, 35 cycles of denaturation at 98°C for 10 sec, annealing at 65°C for 20 sec and extension at 72°C for 7 min. Genomic DNA containing 100 copies of HTLV-1 provirus for the *pX* region from each subject was used. To ensure that same amount of provirus was used for each reaction, PCR for the *pX* region was performed as an internal control. Primers used for this PCR were as follows: the forward primer (HTLV-7396F 5′-GGCGACTGGTGCCCCATCT CTGGGGGACTATGTTCG-3′: positions 7396–7431) and the reverse primer described above (HTLV-8345R).

DNA sequence analysis for Type 1 defective provirus

Long PCR products from subjects suspected of having defective provirus were subcloned by pGEM-T Easy vector system (Promega). The resulting plasmid DNA was purified by GenElute Plasmid Miniprep Kit (Sigma-Aldrich, St. Louis, MO). The DNA sequence of long PCR product was identified using an ABI PRISM Genetic Analyzer 310 (Applied Biosystems).

Southern blot hybridization analysis

To analyze the clonality of HTLV-1-infected cells, Southern blot analysis for HTLV-1 provirus was performed based on the method previously described by Kamihira *et al.* with slight modification.[17] Genomic DNA samples (10 μg) from cases were digested with restriction enzyme *Eco*RI (Fermentas, Barlington, Canada), electrophoresed on 0.7% agarose gel and transferred to nylon membrane (Roche). The filter was hybridized with DIG-PCR-labeled HTLV-1 DNA probe mix, which was prepared by a mixture of PCR products to cover the genome of 5′LTR-*gag* (positions 655–1624), *pro* (positions 2109–2619), *pol* (positions 3410–4059), *env* (positions 5464–6114) and *pX* (positions 7461–8646) and by incorporating DIG-11-dUTP (Roche). Finally, the band patterns were visualized with a CDP-star (Roche).

Results

PVLs of 208 asymptomatic HTLV-1 carriers based on the real-time PCR for the *pol* and *pX* regions

PVLs of 208 asymptomatic HTLV-1 carriers were determined by real-time PCR using primers for the *pol* and *pX* regions. The mean PVLs determined using primers for the *pol* region (2.3 copies per 100 PBMCs) were lower than that for the *pX* region (3.6 copies per 100 PBMCs). Because the *pX* region has been reported to be conserved in the HTLV-1 provirus,[14,16] the carriers, whose PVLs for the *pol* region were much lower than those for the *pX* region, were assumed to have many PBMCs harboring defective HTLV-1 provirus. Therefore, to characterize the carriers with defective HTLV-1 provirus, the subjects with relatively high PVLs for the *pX* region, which were equal to or greater than 1.0 copy per 100 PBMCs, and with PVLs for the *pol* region, which were less than half of those for the *pX* region, were supplied for further analysis. Seven carriers (Cases A–G) among 111 carriers with PVLs for the *pX* region, which were equal to or greater than 1.0 copy per 100 PBMCs, met this condition (Table 1).

DNA polymorphism analysis for the *pol* primer region

Although these seven carriers were potential carriers with relatively high PVLs and defective provirus, there was a possibility that the low PVLs for the *pol* region were due to the polymorphism of the DNA sequence of primers and probe for the *pol* region. Therefore, DNA sequences of the *pol* regions for PCR in Cases A–G were determined by the direct sequencing of PCR products. In Cases A–G, the polymorphism was not detected in the forward primer and probe annealing sequences. However, as shown in Table 1, the polymorphism of the DNA sequence was identified in two positions (3860 A>C and 3876 G>A) of the genome of provirus for the reverse primer for the *pol* region in four of seven cases (Cases D–G, Table 1). This DNA sequence was cloned into the plasmid, and the amplification efficacy of real-time PCR for the *pol* region was assessed. As expected, the amplification efficacy of real-time PCR in the plasmid with two nucleotide substitutions was ~3–4% of that in the plasmid without nucleotide substitutions (data not shown). These results accounted for the low PVLs for the *pol* region in Cases D–G shown in Table 1. Therefore, only Cases A–C were thought to potentially have many PBMCs with defective HTLV-1 provirus.

Sequential change of PVLs determined by real-time PCR for the *pol* and *pX* regions

All of three cases (Cases A, B and C) were followed-up for 10 or more years, and the samples from several screens were available (Fig. 2). None of these cases showed any signs or

Table 1. Proviral DNA loads for the *pol* and *pX* regions and polymorphism found in the *pol* region

Cases	Sex	Age (years)	PVLs (copies/100 PBMCs)			Polymorphism of *pol* region	
			pX	*pol*	*pX/pol*	3860[1]	3876[1]
A	Male	61	57.5	2.8	21.7	A	G
B	Female	73	31.7	0.5	59.2	A	G
C	Female	84	17.3	3.8	4.6	A	G
D	Male	82	12.6	0.4	5.5	C	A
E	Male	45	3.7	0.1	30.6	C	A
F	Male	75	2.5	0.1	27.2	C	A
G	Male	83	1.9	0.1	24.5	C	A

PVLs: proviral DNA loads; PBMCs: peripheral blood mononuclear cells.
[1]Position of proviral genome sequence.

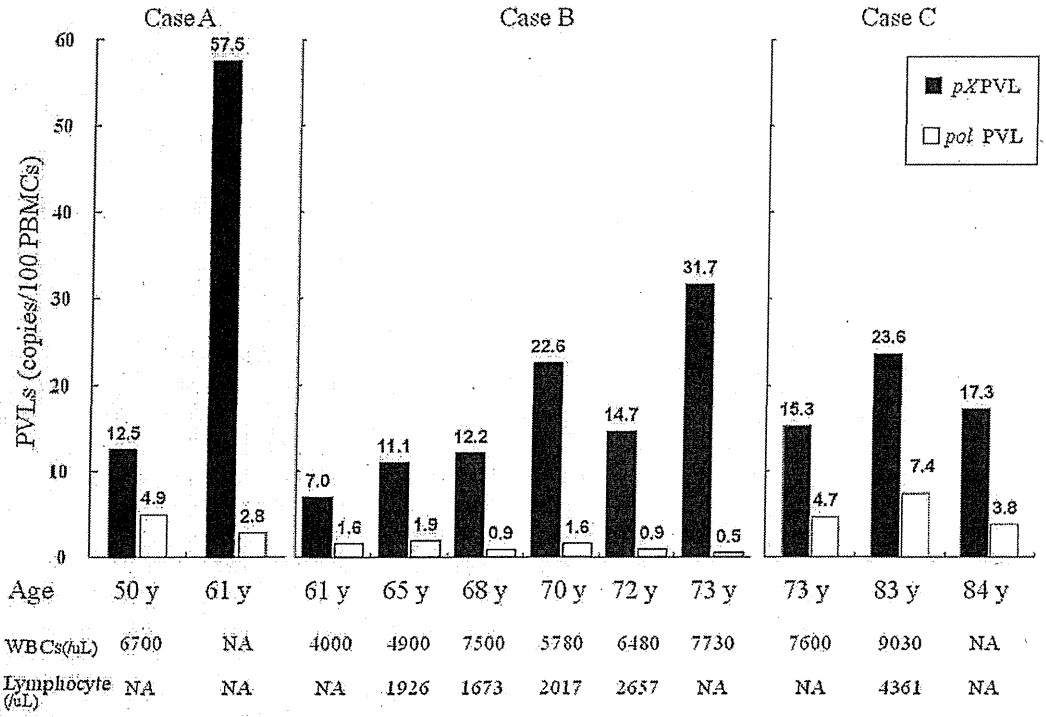

Figure 2. Proviral DNA loads for *pol* and *pX* regions at different ages of Cases A, B and C. WBCs: white blood cells; NA: not available.

symptoms suggesting ATL- and HTLV-1-associated diseases. The numbers of white blood cells and lymphocytes in their peripheral blood were within normal limits with no abnormal cells observed during the follow-up period. Cases A, B and C had high PVLs for the *pX* region, which were greater than 15 copies per 100 PBMCs at the most recent screens, when the cases were 61, 73 and 84 years old, respectively. PVLs for both the *pol* and *pX* regions were measured in previous time-sequential samples from these cases (Fig. 2). PVLs for the *pX* region in Cases A and B showed a marked increase during the 11- and 12-year follow-up, and those for the *pol* region showed either no change or decreased.

Sequencing and analysis for defective provirus in three cases

Long PCR to amplify the HTLV-1 provirus using primers for 5′ LTR and for the *pX* region was performed in the time-sequential samples from Cases A, B and C (Fig. 3). This long PCR amplifies the complete provirus and the Type 1 defective provirus with 5′ LTR conserved. In other words, Type 2 defective provirus, which does not conserve 5′LTR, is not amplified by this long PCR. If the subject had a complete proviral genome, the size of PCR product would be expected to be 7.7 kb. If the PCR products were smaller than 7.7 kb, they were judged to be derived from Type 1 defective provirus.

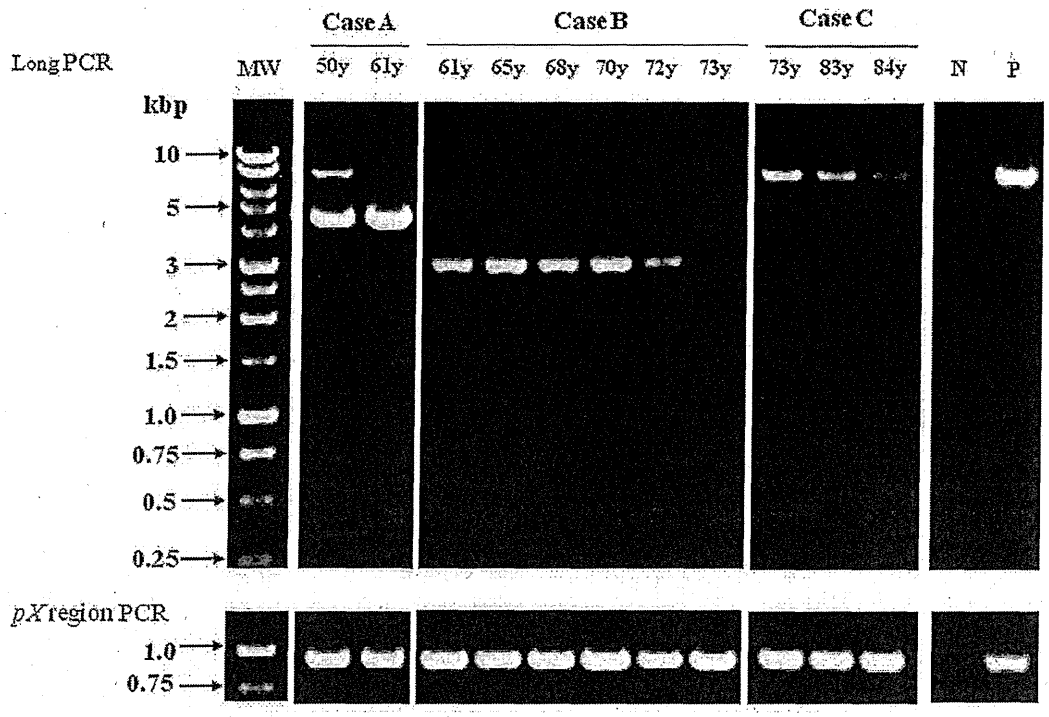

Figure 3. Detection of defective provirus by long polymerase chain reaction at different ages of Cases A, B and C. MW: molecular weight marker; N: human T-lymphotropic virus Type 1 (HTLV-1) negative subject; P: HTLV-1-positive cell line, ED-40515.

In Case A, a strong band of 4.5 kb and a weak band of 2.7 kb were detected in addition to a band of 7.7 kb at age of 50 years. When Case A was 61 years old, the strong 4.5 kb band increased its intensity. In contrast, the weak band of 2.7 kb was not detectable, and the band for the complete proviral genome decreased its intensity. The DNA sequence of the strong band of 4.5 kb showed that this band represented a Type 1 defective provirus with a 3.2-kb deficiency (positions 1203–4368, Fig. 4).

In Case B, a strong band of 2.9 kb was detected in addition to a weak band of 7.7 kb at age of 61 years. The DNA sequence of this 2.9 kb band showed that this band also represented a Type 1 defective provirus with 4.8 kb deficiency (positions 1173–5958, Fig. 4). When Case B was 73 years old, the intensity of the 2.9 kb band decreased markedly (Fig. 3). However, PVLs in Case B gradually increased as time passed (Fig. 2). Therefore, HTLV-1-infected cells harboring 2.9-kb Type 1 defective provirus were assumed not to be responsible for the increase of PVLs in Case B. In other words, HTLV-1-infected cells harboring provirus, which was not detected by long PCR used in our study, increased in number.

In Case C, several bands smaller in size than 7.7 kb, which might represent different Type 1 defective provirus, were detected. However, they were not consistently detectable at the ages of 73, 83 and 84. The 7.7-kb band of the complete proviral genome also decreased its intensity at the age of 84 years. The PCR product at age of 83 years was subcloned, and the DNA sequence was identified (Fig. 4). Thirteen Type 1 defective proviruses were detected in the 33 colonies derived from PCR products except for provirus with complete genome. Four of these were found to have insertions of nonviral sequences (clone cc-1,-3,-4 and -6, in Fig. 4).

Analysis of clonality of HTLV-1-infected cells by Southern blotting

To examine the clonal expansion of HTLV-1-infected cells, samples of genomic DNA (10 μg) from Cases A, B and C were analyzed by Southern blotting (Fig. 5). In Case A, a 17-kb band (a-1) was detected both at 50 and 61 years of age. The intensity of a-1 increased markedly at age 61. The increased intensity of clone a-1was consistent with the finding of increased PVLs for the *pX* region (Fig. 2) and with the increased intensity of the 4.5-kb band of Type 1 defective provirus by long PCR (Fig. 3). In addition, another weak band (a-2) was detected at age 61. Because the size of a-2 was ~7 kb, which was smaller than the size of complete HTLV-1 provirus (9 kb), a-2 was considered to be a clone with defective provirus, which was not detected by long PCR. In Case B, two clones (b-1 and b-2) were detected both at

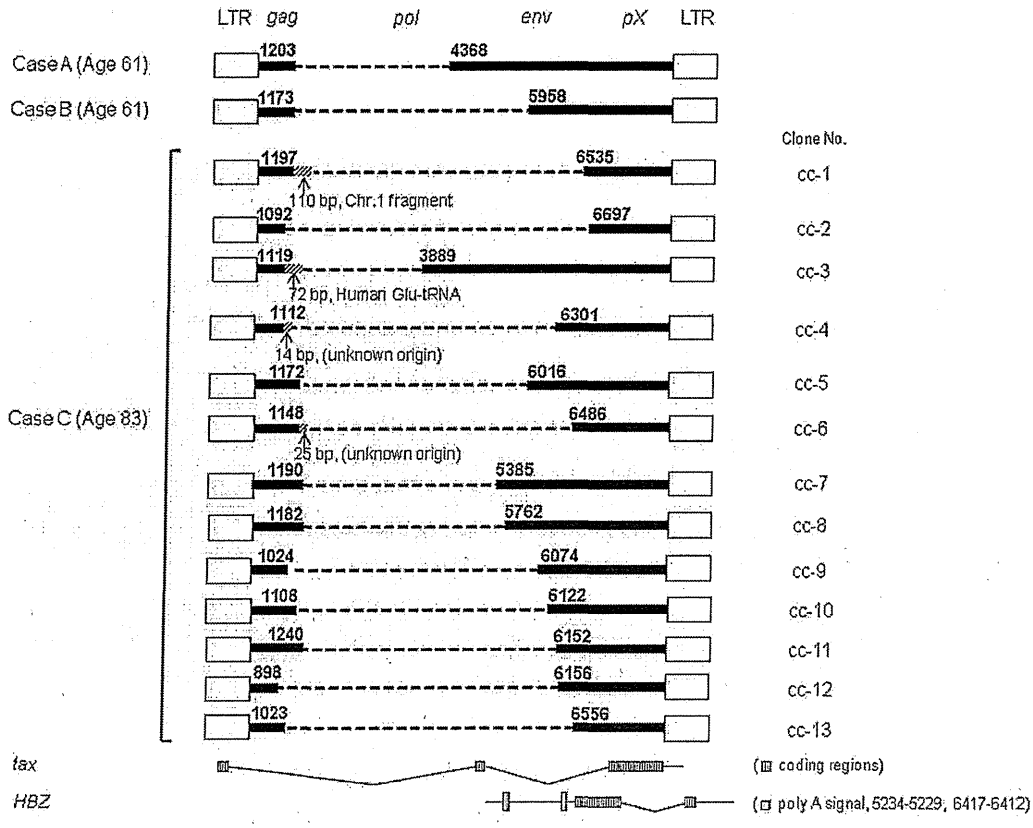

Figure 4. The schema of Type 1 defective provirus in Cases A, B and C. Dotted lines represent the defective regions of provirus. Splicing patterns of *tax* and *HBZ* genes are revealed. The nucleotide position numbers of human T-lymphotropic virus Type 1 (HTLV-1) provirus are same as those of Figure 1.

ages 61 and 70. The intensity of b-2 did not change during 9 years; however, that of b-1 increased at the age of 70. PVLs for the *pX* region increased (Fig. 2); however, the intensity of 2.9-kb Type 1 defective provirus by long PCR showed no change or decreased at age 70 (Fig. 3). Therefore, it was possible that clone b-2 represented the HTLV-1-infected cells with 2.9-kb Type 1 defective provirus detected by long PCR, and that another clone (b-1) of HTLV-1-infected cells with provirus, which was not detectable by long PCR, contributed to the increase of the PVLs in Case B. In Case C, one clone (c-1) was detected both at ages 73 and 84, and the other clone (c-2) was detected only at age 84. The intensity of c-1 was somewhat increased at the age of 84. The size of c-2 was ~7 kb and was considered to be a clone with defective provirus. However, clones c-1 and c-2 were not considered to be harboring Type 1 defective provirus because no band was observed to be increased in intensity at age 84 by long PCR (Fig. 3).

Discussion

To identify asymptomatic carriers, who have PBMCs harboring defective provirus with large deletions, PVLs of 208 asymptomatic HTLV-1 carriers were determined by real-time PCR using primers for the *pol* and *pX* regions. HTLV-1 *pX* region has been reported to be well conserved in the proviral genome.[14,16] Therefore, as expected, PVLs for the *pol* region were lower than those for the *pX* region. The carriers showing PVLs for the *pol* region, which were lower than those for the *pX* region, were considered to be candidates who have many PBMCs harboring defective provirus with large deletions of internal sequences. One hundred and eleven asymptomatic carriers showed relatively high PVLs (equal to or greater than 1.0 copy per 100 PBMCs). Seven showed low PVLs for the *pol* region (less than half of those for the *pX* region) among these 111 carriers. Four cases were excluded from further analysis because their low PVLs for the *pol* region were due to polymorphism of the proviral genome at the site of primer annealing. Three (Cases A, B and C) were considered as candidates for asymptomatic carriers, who have many HTLV-1-infected cells harboring defective provirus with large deletions. PVLs for the *pX* region increased in Cases A and B during follow-up for equal to or greater than 10 years. In contrast, PVLs for the *pol* region showed no change or decreased. These data suggested that the number

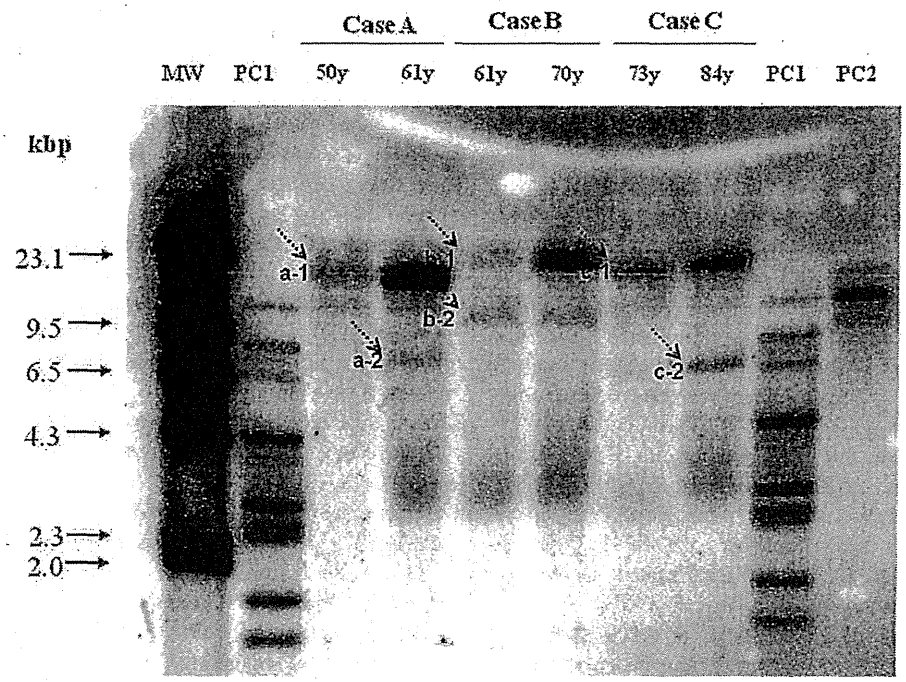

Figure 5. Southern blot analysis for human T-lymphotropic virus Type 1 (HTLV-1) provirus at different ages of Cases A, B and C. Arrows indicate predominant clones of HTLV-1-infected cells. PC1: DNA sample from HTLV-1-positive cell line, ST-1, which was digested with *Pst* I; PC2: DNA sample from HTLV-1-positive cell line, SO_4, which was digested with *Eco* RI; MW: molecular weight marker.

of HTLV-1-infected cells harboring defective provirus increased in Cases A and B.

Then, the defective provirus and the clonality of HTLV-1-infected cells were analyzed for the time-sequential samples from each subject. In Case A, a Type 1 defective provirus with a deletion of internal sequence of 3.2 kb was evident at the age of 50, and its intensity increased at age 61 (Fig. 3). Therefore, the increase of PVLs for the *pX* region, not for the *pol* region, was considered because of the clonal expansion of the HTLV-1-infected cells with this Type 1 defective provirus. Southern blot analysis showing the increased intensity of clone a-1 at age 61 supported this hypothesis. In Case B, a Type 1 defective provirus with the deletion of internal sequence of 4.8 kb was evident at age 61 (Fig. 3). The increase of PVLs for the *pX* region was not explained by the expansion of the HTLV-1-infected cells with this Type 1 defective provirus because the intensity of the PCR product for this defective provirus decreased at ages 72 and 73. Southern blot analysis showed two clones at the age of 61. Clone b-2 showed the same intensity at ages 61 and 70; however, clone b-1 increased in intensity at age 70. Therefore, the HTLV-1-infected cells harboring the Type 1 defective provirus in this case were more likely to belong to clone b-2. The increased PVLs at ages 70–73 were considered to be due to an increased number of HTLV-1-infected cells, which belonged to clone b-1. Clone b-1 was assumed to harbor the defective provirus because only a very weak band for complete provirus was detectable by long PCR in Case B. However, the defective provirus accounting for clone b-1 was not detectable by long PCR and could be a Type 2 defective provirus. Alternatively, a polymorphism of the DNA sequence in the site of primers of long PCR in 5′-LTR for clone b-1 may explain the absence of the band for defective provirus by long PCR. Therefore, it was considered that two major clones with defective provirus existed in Case B at age 61, and only clone b-1 survived as time passed. In Case C, several bands, which may have represented different Type 1 defective provirus, were detected by long PCR in addition to the band for the complete provirus at age 73. These defective proviruses were not consistently detectable at ages 73, 83 and 84. The intensity of the band for the HTLV-1-infected cells with complete provirus was also decreased as time passed. Therefore, maintenance of high PVLs at the age of 84 was not explained by these Type 1 defective proviruses alone. HTLV-1-infected cells with defective provirus, which was not detectable by long PCR in our study, might exist in Case C. In fact, Southern blot analysis showed increased intensity of clone c-1 and the appearance of new clone c-2 at age 84 (Fig. 5). The data from Cases A, B and C in our study suggested that HTLV-1-infected cells with certain types of defective provirus could be the predominant clones and persist for several years; however, the clones of HTLV-1-infected cells do not always survive for a long time in asymptomatic carriers.

Furukawa *et al.* reported that clonally proliferated cells infected with HTLV-1 were detected and were stable for from 4 months to 3 years in patients with HAM/TSP and their seropositive family members without showing any significant indication of ATL.[23] None of Cases A, B and C in our study showed any symptoms and data suggesting ATL- or HTLV-1-associated diseases, even at the end of the follow-up. Therefore, these carriers were judged not to have developed clinical ATL although they had high PVLs and clonal expansion of HTLV-1-infected cells with defective provirus. HTLV-1 Tax protein has been shown to promote the proliferation of infected cells.[13,24] On the other hand, Tax is also reported to be a good target for the host cellular immune response to HTLV-1.[25] HBZ protein was also reported to be important for the proliferation of HTLV-1-infected cells.[26–28] The proviral genome for *HBZ* gene, which is transcribed from 3′LTR, can be conserved even in the Type 2 defective provirus.[16,18] The Type 1 defective provirus found in Case A possessed internal deletion (positions 1203–4368). Theoretically, the expression of Tax and HBZ protein is not prevented by this internal deletion. Therefore, Tax and HBZ may have promoted the proliferation of HTLV-1-infected cells harboring this defective provirus although this proliferation might have been controlled by cytotoxic T-lymphocytes (CTL) through the recognition of Tax. At the same time, this defective provirus cannot express envelope and core proteins, which were also reported as the targets for CTL in HTLV-1 carriers.[29] Therefore, HTLV-1-infected cells harboring this defective provirus may be able to avoid attack from CTL more efficiently. In Case B, Type 1 defective provirus detected by long PCR possessed larger internal deletion (positions 1173–5958). Theoretically, the expression of Tax was prevented because of the deletion of the second exon of the *tax* gene in this defective provirus. It is not clear whether the loss of the expression of Tax protein was related to the decreased intensity of this clone at age 73. Theoretically, this Type 1 defective provirus was able to express HBZ protein because the provirus genome of *HBZ* gene was conserved. In Case C, 13 Type 1 defective proviruses were found at age 83. Twelve among these 13 clones (except clone cc-3 in Fig. 4) had large internal deletions, which theoretically prevent the expression of Tax. Moreover, 4 of 12 clones had the deletions, which theoretically prevent the expression of HBZ protein because of either the deficiencies of the coding regions of *HBZ* and/or deficiencies of two poly A signals (clone cc-1, −2, −6 and −13 in Fig. 4). These large deletions of defective provirus might account for clones not being consistently detectable during a long period in Case C.

In Cases B and C, the increase of PVLs in the time-sequential samples could not be explained by the existence of HTLV-1-infected cells with Type 1 defective provirus. The different clones of HTLV-1-infected cells with defective provirus, which was not detectable by the long-PCR used in our study, might exist in these cases. Clonal expansion of HTLV-1-infected cells with defective provirus, which does not express Tax protein and may not be recognized by the CTL, but which does promote the proliferation of HTLV-1-infected cells under the expression of HBZ protein, was possible. Indeed, HTLV-1-infected cells harboring Type 2 defective provirus were found more frequently in patients with ATL, suggesting a greater potential for leukemogenesis.[17,18]

In Case C, 4 of 13 Type 1 defective proviruses were found to have insertions of nonviral sequences (clone cc-1, −3, −4 and −6 in Fig. 4). Tamiya *et al.* also reported that insertion of a nonviral sequence (35 bp), which was derived from human proline transfer RNA, between the primer binding site and *env* region of HTLV-1 provirus in a patient with ATL.[16] They assumed that this nonviral sequence was inserted into the defective provirus during reverse transcription because human proline transfer RNA had the 16-bp homologous sequence with the 5′-region of HTLV-1. In our study, the DNA sequences of the inserted nonviral sequences in clone cc-1 and −3 were compared to the sequence of the 5′-region of HTLV-1. However, the homologous sequence was not found, and we could not clarify the mechanism of insertions of nonviral sequences in the defective provirus in Case C.

A major limitation of our study is that we were unable to identify genome sequences of Type 2 defective provirus, which possibly existed in Cases B and C, because of technical limitations. Further study to identify Type 2 defective provirus in asymptomatic carriers through improved methodology is necessary. In addition, the number of cases in which defective provirus was analyzed was small in our study. The analysis of more cases may clarify whether the HTLV-1-infected cells harboring the defective provirus have a growth advantage.

In our study, PVLs measured using primers for the *pol* region were less than those for the *pX* region in 208 asymptomatic HTLV-1 carriers. Analysis of seven carriers, who had relatively high PVLs for the *pX* region but much lower PVLs for the *pol* region, showed that they had HTLV-1-infected cells with polymorphism of proviral genome for the *pol* region or with defective provirus. All three asymptomatic HTLV-1 carriers, who had many HTLV-1-infected cells with defective provirus, showed high PVLs. The PVLs in two of the carriers increased markedly after a 10- to 12-year interval. This increase was considered to be due to the expansion of HTLV-1-infected cells with defective provirus. Accordingly, it is suggested that HTLV-1-infected cells with certain types of defective provirus can be predominant clones; however, not all predominant clones of HTLV-1-infected cells survive for a long time. Therefore, the detection of major clones of HTLV-1-infected cells may not always predict the development of ATL. Further study is necessary to clarify whether certain types of defective provirus are related to disease outcome such as ATL.

Acknowledgement

The authors thank Dr. M. Maeda (Kyoto University) for providing ED-40515(−) cell lines.

References

1. Uchiyama T, Yodoi J, Sagawa K, Takatsuki K, Uchino H. Adult T-cell leukemia: clinical and hematologic features of 16 cases. *Blood* 1977;50:481–92.
2. Yoshida M, Miyoshi I, Hinuma Y. Isolation and characterization of retrovirus from cell lines of human adult T-cell leukemia and its implication in the disease. *Proc Natl Acad Sci USA* 1982;79:2031–5.
3. Osame M, Usuku K, Izumo S, Ijichi N, Amitani H, Igata A, Matsumoto M, Tara M. HTLV-I associated myelopathy, a new clinical entity. *Lancet* 1986;1:1031–2.
4. Gessain A, Barin F, Vernant JC, Gout O, Maurs L, Calender A, De Thé G. Antibodies to human T-lymphotropic virus type-I in patients with tropical spastic paraparesis. *Lancet* 1985;24:407–10.
5. Seiki M, Eddy R, Shows TB, Yoshida M. Nonspecific integration of the HTLV provirus genome into adult T-cell leukaemia cells. *Nature* 1984;309:640–2.
6. Arisawa K, Soda M, Endo S, Kurokawa K, Katamine S, Shimokawa I, Koba T, Takahashi T, Saito H, Doi H, Shirahama S. Evaluation of adult T-cell leukemia/lymphoma incidence and its impact on non-Hodgkin lymphoma incidence in southwestern Japan. *Int J Cancer* 2000;85:319–24.
7. Yamaguchi K, Watanabe T. Human T lymphotropic virus type-I and adult T-cell leukemia in Japan. *Int J Hematol* 2002;76:240–5.
8. Wattel E, Vartanian JP, Panneitier C, Wain-Hobson S. Clonal expansion of human T-cell leukemia virus type I-infected cells in asymptomatic carriers without malignancy. *J Virol* 1995;69:2863–8.
9. Etoh K, Tamiya S, Yamaguchi K, Okayama A, Tsubouchi H, Ideta T, Mueller N, Takatsuki K, Matsuoka M. Persistent clonal proliferation of human T-lymphotropic virus type I-infected cells *in vivo*. *Cancer Res* 1997;57:4862–7.
10. Cavrois M, Leclercq I, Gout O, Gessain A, Wain-Hobson S, Wattel E. Persistent oligoclonal expansion of human T-cell leukemia virus type 1-infected circulating cells in patients with Tropical spastic paraparesis/HTLV-1 associated myelopathy. *Oncogene* 1998;17:77–82.
11. Tanaka G, Okayama A, Watanabe T, Aizawa S, Stuver S, Mueller N, Hsieh CC, Tsubouchi H. The clonal expansion of human T lymphotropic virus type 1-infected T cells: a comparison between seroconverters and long-term carriers. *J Infect Dis* 2005;191:1140–7.
12. Okayama A, Stuver S, Matsuoka M, Ishizaki J, Tanaka G, Kubuki Y, Mueller N, Hsieh CC, Tachibana N, Tsubouchi H. Role of HTLV-1 proviral DNA load and clonality in the development of adult T-cell leukemia/lymphoma in asymptomatic carriers. *Int J Cancer* 2004;110:621–5.
13. Yoshida M. Multiple viral strategies of HTLV-1 for dysregulation of cell growth control. *Annu Rev Immunol* 2001;19:475–96.
14. Ohshima K, Kikuchi M, Masuda Y, Kobari S, Sumiyoshi Y, Eguchi F, Mohtai H, Yoshida T, Takeshita M, Kimura N. Defective provirus form of human T-cell leukemia virus type I in adult T-cell leukemia/lymphoma: clinicopathological features. *Cancer Res* 1991;51:4639–42.
15. Korber B, Okayama A, Donnelly R, Tachibana N, Essex M. Polymerase chain reaction analysis of defective human T-cell leukemia virus type I proviral genomes in leukemic cells of patients with adult T-cell leukemia. *J Virol* 1991;65:5471–6.
16. Tamiya S, Matsuoka M, Etoh K, Watanabe T, Kamihira S, Yamaguchi K, Takatsuki K. Two types of defective human T-lymphotropic virus type I provirus in adult T-cell leukemia. *Blood* 1996;88:3065–73.
17. Kamihira S, Sugahara K, Tsuruda K, Minami S, Uemura A, Akamatsu N, Nagai H, Murata K, Hasegawa H, Hirakata Y, Takasaki Y, Tsukasaki K, et al. Proviral status of HTLV-1 integrated into the host genomic DNA of adult T-cell leukemia cells. *Clin Lab Haematol* 2005;27:235–41.
18. Miyazak M, Yasunaga J, Taniguchi Y, Tamiya S, Nakahata T, Matsuoka M. Preferential selection of human T-cell leukemia virus type 1 provirus lacking the 5′ long terminal repeat during oncogenesis. *J Virol* 2007;81:5713–23.
19. Morozov VA, Lagaye S, Taylor GP, Matutes E, Weiss RA. Chimeric matrix proteins encoded by defective proviruses with large internal deletions in human T-cell leukemia. *J Virol* 2000;74:3933–40.
20. Mueller N, Okayama A, Stuver S, Tachibana N. Findings from the Miyazaki Cohort Study. *J Acquir Immune Defic Syndr Hum Retrovirol* 1996;13–1:S2–S7.
21. Seiki M, Hattori S, Hirayama Y, Yoshida M. Human adult T-cell leukemia virus: complete nucleotide sequence of the provirus genome integrated in leukemia cell DNA. *Proc Natl Acad Sci USA* 1983;80:3618–22.
22. Takajo I, Umeki K, Morishita K, Yamamoto I, Kubuki Y, Hatakeyama K, Kataoka H, Okayama A. Engraftment of peripheral blood mononuclear cells from human T-lymphotropic virus Type 1 carriers in NOD/SCID/γ^{null} (NOG) Mouse. *Int J Cancer* 2007;121:2205–11.
23. Furukawa Y, Fujisawa J, Osame M, Toita M, Sonoda S, Kubota R, Ijichi S, Yoshida M. Frequent clonal proliferation of human T-cell leukemia virus type 1 (HTLV-1)-infected T cells in HTLV-1-associated myelopathy (HAM-TSP). *Blood* 1992;80:1012–16.
24. Franchini G. Molecular mechanisms of human T-cell leukemia/lymphotropic virus type I infection. *Blood* 1995;86:3619–39.
25. Kannagi M, Harada S, Maruyama I, Inoko H, Igarashi H, Kuwashima G, Sato S, Morita M, Kidokoro M, Sugimoto M, Funahashi S, Osame M, et al. Predominant recognition of human T cell leukemia virus type I (HTLV-I) *pX* gene products by human CD8+ cytotoxic T cells directed against HTLV-I-infected cells. *Int Immunol* 1991;3:761–7.
26. Satou Y, Yasunaga J, Yoshida M, Matsuoka M. HTLV-I basic leucine zipper factor gene mRNA supports proliferation of adult T cell leukemia cells. *Proc Natl Acad Sci USA* 2006;103:720–5.
27. Arnold J, Yamamoto B, Li M, Phipps AJ, Younis I, Lairmore MD, Green PL. Enhancement of infectivity and persistence in vivo by HBZ, a natural antisense coded protein of HTLV-1. *Blood* 2006;107:3976–82.
28. Murata K, Hayashibara T, Sugahara K, Uemura A, Yamaguchi T, Harasawa H, Hasegawa H, Tsuruda K, Okazaki T, Koji T, Miyanishi T, Yamada Y, et al. A novel alternative splicing isoform of human T-cell leukemia virus type 1 bZIP factor (HBZ-SI) targets distinct subnuclear localization. *J Virol* 2006;80:2495–505.
29. Kannagi M. Immunologic control of human T-cell leukemia virus type I and adult T-cell leukemia. *Int J Hematol* 2007;86:113–17.

Leukemia (2011) 25, 921–931

www.nature.com/leu

ORIGINAL ARTICLE

CD52 as a molecular target for immunotherapy to treat acute myeloid leukemia with high EVI1 expression

Y Saito, S Nakahata, N Yamakawa, K Kaneda, E Ichihara, A Suekane and K Morishita

Department of Medical Science, Division of Tumor and Cellular Biochemistry, Faculty of Medicine, University of Miyazaki, Miyazaki, Japan

Ecotropic viral integration site 1 (EVI1) is an oncogenic transcription factor in human acute myeloid leukemia (AML) with chromosomal alterations at 3q26. Because a high expression of EVI1 protein in AML cells predicts resistance to chemotherapy with a poor outcome, we have searched for molecular targets that will treat these patients with AML. In this study, we determined that CD52, which is mainly expressed on lymphocytes, is highly expressed in most cases of AML with a high EVI1 expression (EVI1^{High}). CAMPATH-1H, a humanized monoclonal antibody against CD52, has been used to prevent graft-versus-host disease and treat CD52-positive lymphoproliferative disorders. Here, we investigated the antitumor effect of CAMPATH-1H on EVI1^{High} AML cells. CAMPATH-1H significantly inhibited cell growth and induced apoptosis in CD52-positive EVI1^{High} leukemia cells. Furthermore, CAMPATH-1H induced complement-dependent cytotoxicity and antibody-dependent cellular cytotoxicity against CD52-positive EVI1^{High} leukemia cells. After an intravenous injection of CAMPATH-1H into NOD/Shi-scid/IL-2Rγ;null mice with subcutaneous engraftment of EVI1^{High} leukemia cells, tumor growth rates were significantly reduced, and the mice survived longer than those in the phosphate-buffered saline-injected control group. Thus, CAMPATH-1H is a potential therapeutic antibody for the treatment of patients with EVI1^{High} leukemia.
Leukemia (2011) **25,** 921–931; doi:10.1038/leu.2011.36; published online 11 March 2011
Keywords: CD52; CAMPATH-1H; EVI1; acute myeloid leukemia

Introduction

Murine ecotropic viral integration site 1 (EVI1) was first identified as a leukemia-associated gene activated by murine retroviral integration.[1,2] A high expression of the human homologue EVI1 is found in 5–10% of patients with acute myeloid leukemia (AML), but chromosome 3q26 abnormalities near the *EVI1* gene are only detected in 1–3% of all AML cases.[3–5] Because AML patients with a high EVI1 expression (EVI1^{High}) had a significantly reduced overall survival, overexpression of the *EVI1* gene is thought to be a poor prognostic factor for AML patients.[6,7] Patients with EVI1^{High} AML often do not respond to chemotherapy and hematopoietic cell transplantation;[8] therefore, identifying novel molecular targets in EVI1^{High} AML is of particular importance. In this study, we identified CD52 as a new surface molecule highly expressed on most EVI1^{High} leukemia cells by DNA microarray, reverse-transcription polymerase chain reaction (RT-PCR) and flow cytometry analyses.

Correspondence: Dr K Morishita, Division of Tumor and Cellular Biochemistry, Department of Medical Science, Faculty of Medicine, University of Miyazaki, 5200 Kihara, Kiyotake-cho, Miyazaki 889-1692, Japan.
E-mail: kmorishi@med.miyazaki-u.ac.jp
Received 11 October 2010; revised 15 December 2010; accepted 21 December 2010; published online 11 March 2011

Human CD52 is a glycosylphosphatidylinositol-anchored antigen expressed on the cell surfaces of normal and malignant lymphocytes.[9–11] Although the function of CD52 is largely unknown, CD52 is a favored target for lymphoma therapy and immunosuppression before bone marrow transplantation.[12–15] Alemtuzumab (CAMPATH-1H; Genzyme, Cambridge, MA, USA) is a recombinant humanized monoclonal antibody targeting the CD52 antigen.[16,17] The binding of CAMPATH-1H to CD52 on lymphocytes induces complement-dependent cytotoxicity (CDC),[18,19] antibody-dependent cell-mediated cytotoxicity (ADCC)[20–22] and direct cytotoxicity.[23,24] Here, we examined the cytotoxic effects of CAMPATH-1H on EVI1^{High} leukemia cells *in vitro* and the effects of CAMPATH-1H treatment on tumor growth in immunodeficient NOD/Shi-scid/IL-2Rγnull (NOG) mice xenografted with EVI1^{High} leukemia cells. Because CAMPATH-1H showed a direct cytotoxic effect, CDC and ADCC activity, as well as an *in vivo* antitumor effect against EVI1^{High} AML cells, CAMPATH-1H is likely to be a good therapeutic agent for AML with EVI1^{High} expression.

Materials and methods

Cell lines

UCSD/AML1 (refs 25, 26) cells derived from human AML were cultured in RPMI 1640 medium (Wako, Osaka, Japan) supplemented with 10% fetal bovine serum and 1 ng/ml granulocyte–macrophage colony-stimulating factor. Seven cell lines, U937 (ref. 27), K562 (ref. 28), KG-1 (ref. 29), HEL (ref. 30), HL60 (ref. 31), THP-1 (ref. 32) and HNT-34 (ref. 33), were purchased from the RIKEN Cell Bank (Tsukuba, Japan). MOLM1 (ref. 34) was purchased from the Hayashibara Institute (Okayama, Japan). Kasumi-3 (refs. 35, 36) was kindly provided by Dr Asoh (Hiroshima University, Hiroshima, Japan). K051 and K052 (ref. 37) were kindly provided by Dr Nomura (Nippon Medical School, Tokyo, Japan). NH was kindly provided by Dr Suzukawa (University of Tsukuba, Tsukuba, Japan). FKH-1 (ref. 38) and OIH-1 (ref. 39) were kindly provided by Dr Hamaguchi (Musashino Red Cross Hospital, Tokyo, Japan). U937, K562, HL60, THP-1, K051, K052, NH, HNT-34, MOLM1 and Kasumi-3 were cultured in RPMI 1640 medium (Wako) supplemented with 10% fetal bovine serum. The UCSD/AML1, MOLM-1, HNT-34 and Kasumi-3 cell lines each have chromosome 3q26 abnormalities with an EVI1^{High}, whereas U937, K562, KG-1, HEL, HL-60, THP-1, K051, K052, NH, FKH-1 and OIH-1 do not have 3q26 abnormalities and show a low EVI1 expression (Supplementary Table 1).

Patient samples

Leukemia cells were obtained from the peripheral blood (PB) of AML patients who had a blast population of more than 80% in

their PB at diagnosis before chemotherapy (Supplementary Table 2). After Ficoll–Hypaque (Sigma, Saint Louis, MO, USA) separation of the PB, the purity of the blast cells was confirmed by flow cytometry using immunofluorescence staining of phycoerythrin-conjugated CD11b and CD33 (Supplementary Figure S2). The study was approved by the Institutional Review Board of the Faculty of Medicine, University of Miyazaki. Informed consent was obtained from all blood and tissue donors according to the Declaration of Helsinki.

Antibodies

The human monoclonal antibody CAMPATH-1H that recognizes CD52 was obtained from Bayer Schering Pharma AG (Berlin-Wedding, Germany). The antibody against caspase-3 was commercially obtained from Cell Signaling Technologies (Beverly, MA, USA; catalog no. 9251).

Oligonucleotide microarray

The protocol used for the sample preparation and microarray processing is available from Affymetrix (Santa Clara, CA, USA). Briefly, at least 5 μg of purified RNA was reverse transcribed using Superscript II reverse transcriptase (Life Technologies, Grand Island, NY, USA) with the primer T7-dT24 containing a T7 RNA polymerase promoter. After a second strand of cDNA was synthesized with RNase H, *Escherichia coli* DNA polymerase and *E. coli* DNA ligase, the cDNA was transcribed *in vitro* to produce biotin-labeled cRNA with a MEGAscript High Yield Transcription Kit (Ambion, Austin, TX, USA) as recommended by the manufacturer. After the cRNA was linearly amplified with T7 polymerase, the biotinylated cRNA was cleaned with an RNeasy Mini Column Kit (Qiagen, Valencia, CA, USA), fragmented to 50–200 nucleotides, and then hybridized to the Affymetrix Human Genome U133 Plus 2.0 Array. The stained microarray was scanned with a GeneArray Scanner (Affymetrix) and the intensity of the signal was calculated with Affymetrix software, Microarray Suite 5.0. All data were scaled with the global scaling method to adjust the target intensity to 300. Then, we chose those genes with at least a 10-fold increase in the expression of the EVI1^{High} AML cells compared with low levels of EVI1 (EVI1^{Low}) AML cells with a statistical significance of P less than 0.01 by the t-test.

Reverse-transcription polymerase chain reaction

The levels of CD52, EVI1 and β-actin mRNA in the AML cells were measured by RT-PCR. Briefly, total RNA was extracted using Trizol (Invitrogen, Carlsbad, CA, USA), and 1 mg of total RNA was reverse-transcribed to obtain first-strand cDNA using an RNA-PCR kit (Takara-Bio Inc., Tokyo, Japan). cDNA fragments were amplied by PCR using specic primers. The primers used were as follows: CD52 forward, 5′-CATCAGCCTC CTGGTTATGG-3′, reverse, 5′-AAATGCCTCCGCTTATGTTG-3′; EVI1 forward, 5′-CACATTCGCTCTCAGCATGT-3′, reverse, 5′-ATTTGGGTTCTGCAATCAGC-3′; and β-actin forward, 5′-G ACAGGATGCAGAAGGAGATTACT-3′, reverse, 5′-TGATCCA CATCTGCTGGAAGGT-3′.

Establishment of stable U937 cell lines expressing EVI1

pGCDMsam-EVI1-IRES-EGFP was kindly provided by Dr A Iwama (Chiba University, Chiba, Japan). To produce recombinant retrovirus, the plasmid DNA was transfected into 293gp cells along with the vesicular stomatitis virus G expression plasmid by $CaPO_4$ co-precipitation. For retroviral transduction, 1×10^5 U937 cells were plated in 96-well flat-bottomed plates and were infected with either an EVI1 retroviral supernatant (pGCDMsam-EVI1-IRES-EGFP) or a mock retroviral supernatant (pGCDMsam-IRES-EGFP) with 100 ng/ml polybrene for 24 h. After 7 days, green fluorescent protein-positive U937 cells were sorted with a JSAN cell sorter (Bay Bioscience, Kobe, Japan).

Establishment of stable UCSD/AML1 cell lines expressing shEVI1

A DNA-based small hairpin (sh) RNA expression vector (pSIREN-retroQ-ZsGreen plasmid; Takara-Bio, Inc.) was used in the EVI1 knockdown experiment. The following sequence was cloned into the *Bam*HI–*Eco*RI site of the plasmid to create an shRNA against human EVI1: (ref. 22) 5′-GATCGCTCTAAGG CTGAACTAGCAGTTCAAGAGACTGCTAGTTCAGCCTTAGATT TTTTG-3′. A pSIREN-retroQ-ZsGreen-shLuc plasmid containing shRNA against luciferase (Takara-Bio Inc.) was used as a control. Retroviral particles were generated using the p10A1 packaging vector (Takara-Bio Inc.) and transient transfection of the 293T cell line, which was carried out with a Hilymax liposome transfection reagent (Dojindo, Kumamoto, Japan). For retroviral infection, 1×10^6 UCSD/AML1 cells were placed in 6 cm dishes containing 5 ml of retroviral supernatant with 100 ng/ml polybrene for 24 h. ZsGreen-positive UCSD/AML1 cells were sorted with a JSAN cell sorter (Bay Bioscience) 2 weeks after viral infection. The repression of EVI1 expression was confirmed by RT-PCR as described above.

Flow cytometry analysis

The cells were stained with the biotinylated CAMPATH-1H on ice for 15 min. They were washed and then labeled with a phycoerythrin-labeled streptavidin antibody on ice for 15 min. After washing, the treated cells were analyzed on a FACScan (Becton Dickinson, San Jose, CA, USA).

Cell growth inhibition assay

Leukemia cells (2×10^5 cells per ml) were incubated with various concentrations of CAMPATH-1H in complete medium at 37 °C in 5% CO_2. The cell growth was evaluated with the Trypan blue exclusion assay. The live cells were enumerated after Trypan blue staining using light microscopy.

Apoptosis assay

Apoptosis assays were performed using the Apoptosis Detection kit (MBL, Nagoya, Japan) according to the manufacturer's protocol. UCSD/AML1, HNT-34 or PT8 cells (2×10^5 cells per ml) were incubated with CAMPATH-1H (10 μg/ml) in complete medium at 37 °C in 5% CO_2 for 48 h. The cells were washed and resuspended in binding buffer at a concentration of 1×10^6 cells per ml. The suspension was then incubated with 5 μl of Annexin-V and 5 μl of propidium iodide for 15 min at room temperature in the dark. Samples were analyzed using a FACScan (Becton Dickinson). Annexin-V-positive cells were considered apoptotic.

Cytotoxicity assays

The CDC and ADCC activities of CAMPATH-1H were measured by a lactate dehydrogenase (LDH)-releasing assay using a cytotoxicity detection kit (Roche, Indianapolis, IN, USA). EVI1^{High} AML cells (1×10^4) were incubated with various concentrations of CAMPATH-1H and human serum as the

source of complement at a dilution of 1:6 (for the CDC assay) or with human PB mononuclear cells as effector cells (effector: target, 50:1 for the ADCC assay) in supplemented RPMI 1640 at 37 °C in 96-well flat-bottomed plates. After an additional incubation for 4 h at 37 °C, the extent of cell lysis was determined by measuring the amount of LDH released into the culture supernatant. The maximum LDH release was determined for cells lysed with 2% Triton X-100. The percentage of specific lysis was calculated according to the following formula: CDC % specific lysis = $100 \times (E-S)/(M-S)$, where E is the absorbance of the experimental well, S is the absorbance in the absence of monoclonal antibody (cells were incubated with medium and complement alone) and M is the maximum release of target cells (activity released from target cells lysed with 2% Triton X-100); ADCC % specific lysis = $100 \times (E-S_E-S_T)/(M-S_E)$, where E is the experimental release (supernatant activity from target cells incubated with antibody and effector cells), S_E is the spontaneous release in the presence of effector cells with antibody (supernatant activity from target cells incubated with effector cells), S_T is the spontaneous release of target cells (supernatant activity from target cells incubated with medium alone) and M is the maximum release of target cells (activity released from target cells lysed with 2% Triton X-100).

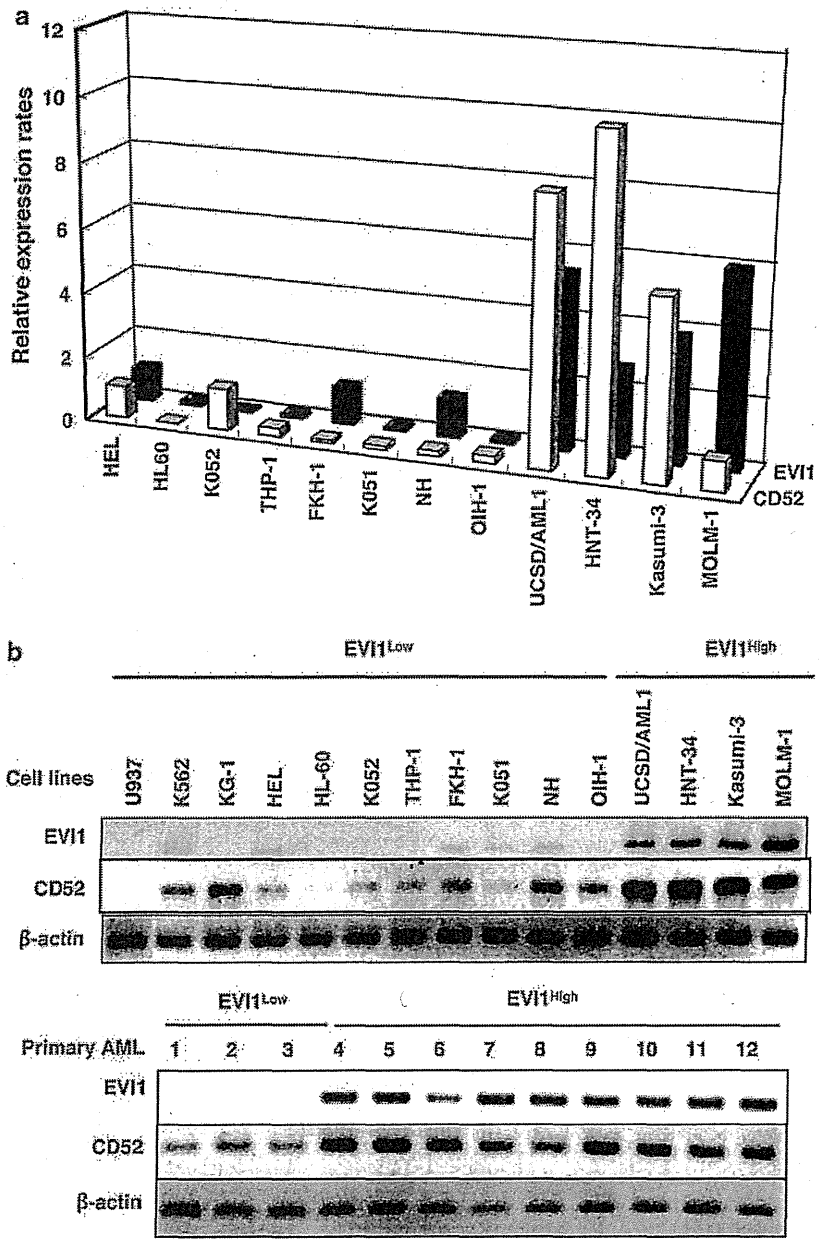

Figure 1 CD52 is highly expressed in EVI1^{High} myeloid leukemia cells. (**a**) The expression profiles of CD52 mRNA by DNA microarray. RNA samples from eight EVI1^{Low} and four EVI1^{High} AML cell lines were used for determining the gene expression profiles. (**b**) Semiquantitative RT-PCR analysis for EVI1 and CD52 is shown for 11 EVI1^{Low} and four EVI1^{High} AML cell lines (top panel), as well as primary AML cells from three patients with EVI1^{Low} and from nine patients with EVI1^{High} expression (bottom panel). The expression of β-actin is shown at the bottom as a control.

Xenograft tumors

Six- to eight-week-old female NOG mice were given a single subcutaneous injection of 5×10^6 UCSD/AML1 cells suspended in 100 µl phosphate-buffered saline (PBS) and mixed with an equal volume of Matrigel (BD Matrigel, BD Biosciences, Bedford, MA, USA). Xenografts were allowed to establish to an average size of 50–100 mm^3, after which mice were randomized into two groups. The groups of mice were given either PBS or CAMPATH-1H at a dose of 100 µg weekly intravenously for 4 weeks. Tumor volumes were derived as the product of the length, width and height of the tumor measured once a week with a caliper. A Kaplan–Meier survival analysis was performed using StatView (SAS Institute, Cary, NC, USA).

Data analysis

A faculty statistician analyzed the data. *P*-values were calculated using the Student's *t*-test for a comparison of independent data sets. Differences were considered statistically significant if the *P*-value was less than 0.05.

Results

EVI1^{High} myeloid leukemia cells express high levels of CD52

To search for novel molecular targets in refractory myeloid leukemia with EVI1^{High}, we initially analyzed the gene expression profiles of 12 human myeloid cell lines using an oligonucleotide microarray (Human Genome U133 Plus 2. 0 Array; Affymetrix) containing 38 500 genes. Four cell lines with chromosome 3q26 abnormalities (UCSD/AML1, HNT-34, Kasumi-3 and MOLM-1) expressed EVI1^{High}, and eight myeloid cell lines without chromosome 3q26 abnormalities (HEL, HL-60, K052, THP-1, FKH-1, K051, NH and OIH-1) expressed EVI1^{Low} (Figure 1a). When the expression profiles between EVI1^{High} and EVI1^{Low} leukemia cell lines were compared, we detected 26 genes that were upregulated over 10-fold in EVI1^{High} leukemia cells when compared with EVI1^{Low} leukemia cells ($P<0.01$) (Table 1). Among these genes, nine genes encode membrane proteins containing extracellular domains. These genes include the CD52 antigen (CAMPATH-1 antigen).

Table 1 Highly expressed genes in EVI1^{High} AML cells compared with EVI1^{Low} AML cells

Gene symbol	*Description*	*Fold change*	*Localization*
EVA1	*Epithelial V-like antigen 1*	54.98	Membrane/extracellular
MMRN1	*Multimerin 1*	49.34	Membrane/extracellular
LOC284262	*Hypothetical protein LOC284262*	47.46	Unknown
EHD2	*EH-domain containing 2*	44.45	Membrane/nucleus
SETBP1	*SET-binding protein 1*	40.48	Nucleus
CALCRL	*Calcitonin receptor-like*	38.95	Membrane/extracellular
CLEC7A	*C-type lectin domain family 7, member A*	32.33	Cytoplasm/membrane
PTPRM	*Protein tyrosine phosphatase, receptor type, M*	26.07	Membrane/extracellular
LCK	*Lymphocyte-specific protein tyrosine kinase*	24.61	Kinase/cytoplasm
ITGA6	*Integrin, alpha 6*	23.83	Membrane/extracellular
CD52	*CD52 antigen (CAMPATH-1 antigen)*	19.35	Membrane/extracellular
DEPDC2	*DEP domain containing 2*	18.45	Intracellular
PTRF	*Polymerase I and transcript release factor*	17.28	Intracellular
S100Z	*S100 calcium-binding protein, zeta*	16.21	Intracellular
RASGEF1B	*RasGEF domain family, member 1B*	14.88	Intracellular
GPR56	*G-protein-coupled receptor 56*	13.98	Membrane/extracellular
PHLDA2	*Pleckstrin homology-like domain, family A, member 2*	13.88	Intracellular
CD300A	*CD300A antigen*	13.08	Membrane/extracellular
TRPS1	*Trichorhinophalangeal syndrome I*	12.55	Nucleus
DPP4	*Dipeptidylpeptidase 4 (CD26, adenosine deaminase complexing protein 2)*	12.07	Membrane/cytoplasm
TNFSF8	*Tumor necrosis factor (ligand) superfamily, member 8*	11.89	Membrane/extracellular
FLJ11996	*Hypothetical protein FLJ11996*	11.48	Unknown
GNGT2	*Guanine nucleotide-binding protein (G protein), gamma-transducing activity polypeptide 2*	11.03	Membrane/cytoplasm
MFAP3L	*Microfibrillar-associated protein 3-like*	10.98	Membrane/extracellular
SYTL4	*Synaptotagmin-like 4 (granuphilin-a)*	10.27	Secretion

Abbreviations: AML, acute myeloid leukemia; EVI1, ecotropic viral integration site 1.
A list of genes that were selected by expression levels greater than 100 and an over 10-fold increased expression in EVI1^{High} AML cells than that in EVI1^{Low} AML cells with significant differences ($P<0.01$). Fold changes were calculated by the mean expression values of EVI1^{High} AML cells compared with EVI1^{Low} AML cells.

Figure 2 EVI1-dependent expression of CD52 in AML cells. (**a**) The expression of CD52 on various leukemic cells by flow cytometry using CAMPATH-1H. Cells were stained with phycoerythrin-labeled CAMPATH-1H, followed by analysis in an FACS. Figures show representative FACS histogram profiles of normal lymphocytes (PBL) and B lymphoid leukemia cell lines (BALL1 and RAMOS) in the upper panel, EVI1^{Low} AML cell lines (U937, NH and K562) in the second panel, EVI1^{High} AML cell lines (UCSD/AML1, HNT-34, Kasumi-3 and MOLM1) in the third panel and primary leukemic cells from patients with EVI1^{Low} (PT1) or EVI1^{High} (PT8, PT9 and PT11) AML in the bottom panel. Open histograms represent cells stained with isotype IgG controls and filled histograms indicate cells stained with CAMPATH-1H. (**b**, **c**) The induction of CD52 expression by a forced expression of EVI1 in U937 with EVI1^{Low} expression. Panel b shows the expression level of CD52 in parental, mock or EVI1 transfectant U937 cells by RT-PCR, and panel c shows the CD52 expression by FACS analysis. (**d**, **e**) The introduction of the shEVI1 expression vector in UCSD/AML1 cells with EVI1^{High} expression decreases CD52 expression. Panel d shows the CD52 mRNA level in parental, control shLuc or shEVI1 transfectant UCSD/AML1 cells by RT-PCR, and panel e shows the CD52 expression by FACS analysis.

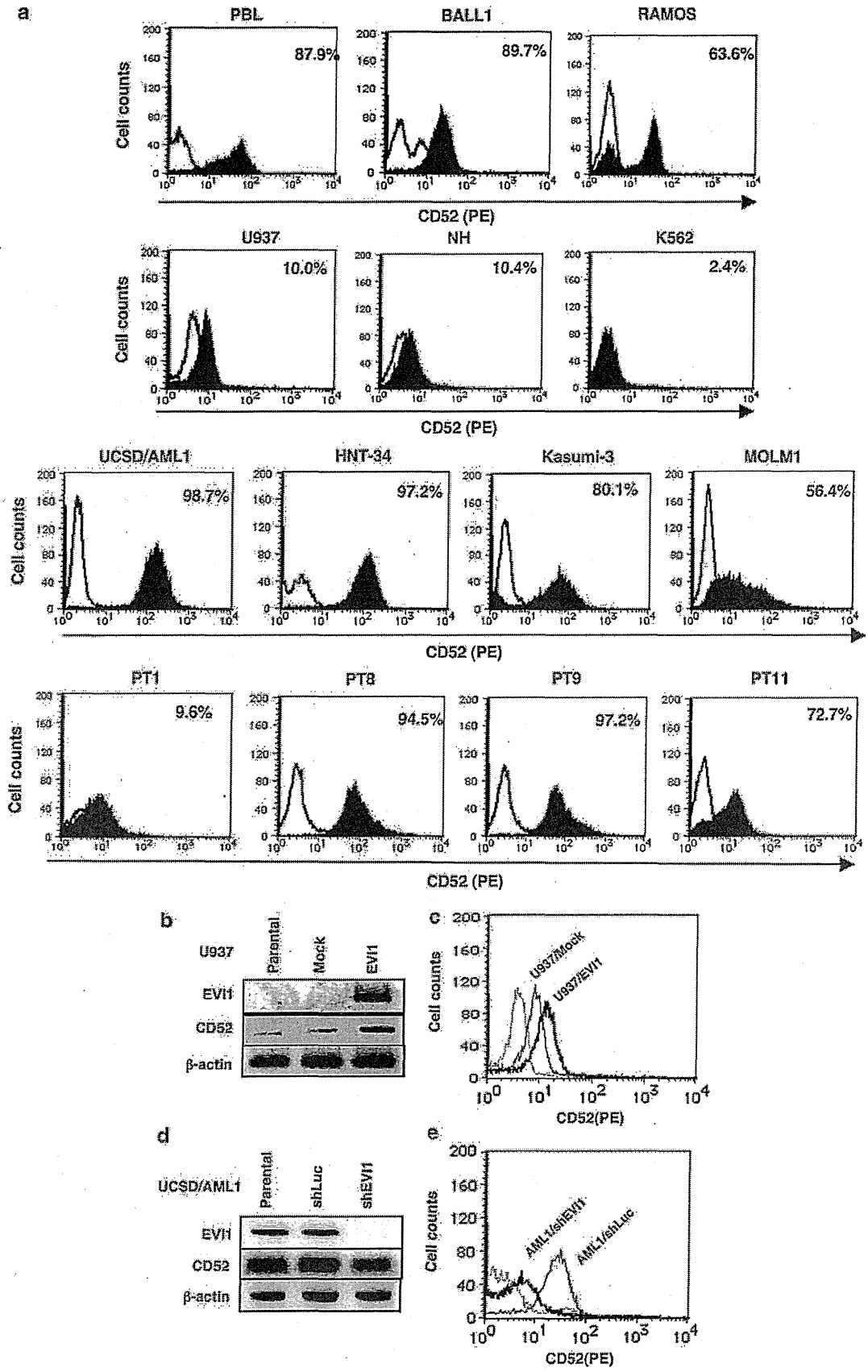
a
PBL
87.9%
BALL1
89.7%
RAMOS
63.6%
U937
10.0%
NH
10.4%
K562
2.4%
UCSD/AML1
98.7%
HNT-34
97.2%
Kasumi-3
80.1%
MOLM1
56.4%
PT1
9.6%
PT8
94.5%
PT9
97.2%
PT11
72.7%
Cell counts
CD52 (PE)
b
U937
Parental
Mock
EVI1
EVI1
CD52
β-actin
c
U937/Mock
U937/EVI1
Cell counts
CD52(PE)
d
UCSD/AML1
Parental
shLuc
shEVI1
EVI1
CD52
β-actin
e
AML1/shEVI1
AML1/shLuc
Cell counts
CD52(PE)

A microarray analysis of the samples from the EVI1^{High} AML cells versus the EVI1^{Low} AML cells confirmed upregulation of CD52 in the EVI1^{High} AML cells (Supplementary Figure S1). Because a humanized anti-CD52 antibody, CAMPATH-1H, has already been developed for immunosuppression before bone marrow transplantation and for gene-targeted therapy for

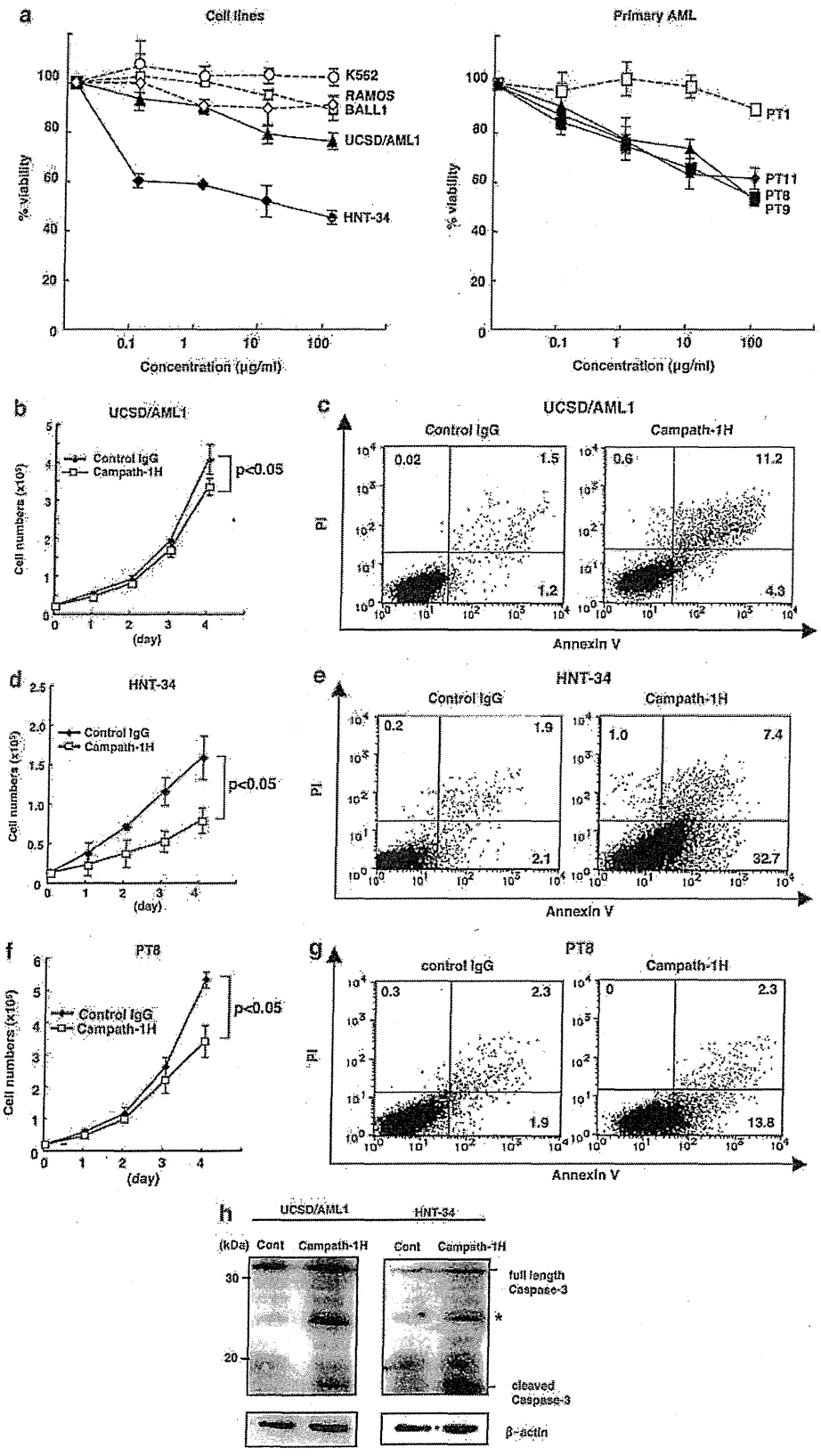

lymphoproliferative disorders, we further analyzed whether the CD52 antigen is a novel target in EVI1^{High} AML.

In the next experiment, CD52 expression was examined in 15 myeloid leukemia cell lines and primary leukemia cells from 12 patients with AML using RT-PCR. We included three additional cell lines without chromosome 3q26 abnormalities (U937, K562 and KG-1) in the analysis. The CD52 expression levels in four cell lines with EVI1^{High} expression (UCSD/AML1, HNT-34, Kasumi-3 and MOLM-1) were higher than that in the other 11 cell lines with EVI1^{Low} expression (Figure 1b, top). In primary leukemia cells, EVI1 and CD52 were more highly expressed in nine patients with chromosome 3q26 abnormalities than that in three patients without chromosome 3q26 abnormalities (Figure 1b, bottom). Thus, CD52 may be a potential marker for EVI1^{High} myeloid leukemia cells.

CAMPATH-1H identifies the CD52 antigen on the surface of EVI1^{High} myeloid leukemia cells

Next, we determined the surface expression of the CD52 antigen by FACS analysis using phycoerythrin-labeled CAMPATH-1H (Figure 2a). We used control PB lymphocytes from a healthy volunteer and two B lymphoid leukemia cell lines (BALL1 and RAMOS) as positive controls and 63.6–89.7% of these cells were labeled by CAMPATH-1H. In EVI1^{Low} myeloid leukemia cell lines (U937, NH and K562) and primary AML cells from a patient with EVI1^{Low} (PT1), 2.4–10.4% of the cells were labeled by CAMPATH-1H with a low signal intensity. In contrast, 56.4–98.7% of EVI1^{High} myeloid leukemic cells (UCSD/AML1, HNT-34, Kasumi-3 and MOLM1) were robustly labeled by CAMPATH-1H, yielding higher signal intensity than BALL1 and RAMOS cells. Moreover, CAMPATH-1H bound to the majority of leukemia cells from three AML patients with inv(3)(q21q26) (PT8 and PT9) or with t(3;21)(q26;q22) (PT11) at a high signal intensity similar to EVI1^{High} cell lines.

To determine whether the EVI1 transcription factor activates CD52 gene expression, we introduced an EVI1 expression vector into an EVI1^{Low} leukemia cell line, U937, and an shRNA targeting EVI1 (shEVI1) into an EVI1^{High} leukemia cell line, UCSD/AML1. After introducing the EVI1 expression vector into U937 cells, the expression of EVI1 was clearly detected in U937/EVI1 cells by RT-PCR, and the level of CD52 mRNA was also increased in U937/EVI1 cells in comparison with parental or mock vector-transfected cells (Figure 2b). FACS analysis showed that the population of CD52-positive cells was increased (61.1%) in U937/EVI1 cells in comparison to U937/mock cells (19.3%), with increased fluorescence intensity (Figure 2c). Moreover, after the introduction of shEVI1 or shRNA against luciferase (shLuc) as a control into UCSD/AML1 cells, the expression level of CD52 mRNA was decreased in UCSD/AML1/shEVI1 cells, along with a decreased expression of EVI1, when compared with parental or UCSD/AML1/shLuc cells (Figure 2d). FACS analysis showed that the percentage of CD52-positive cells in AML1/shEVI1 cells was considerably lower (24.0%) than that in AML1/shLuc (45.1%) cells with decreased fluorescence (Figure 2e). Thus, the CD52 expression in myeloid leukemic cells is partly dependent on the expression of EVI1, and CD52 may be one of the downstream target genes regulated directly or indirectly by EVI1.

CAMPATH-1H induced a direct cytotoxic effect on EVI1^{High} AML cells

Because CAMPATH-1H was highly reactive with the surface of EVI1^{High} AML cells, it may be a good therapeutic candidate for EVI1-positive AML. We initially tested the growth inhibitory and direct cytotoxic effects of CAMPATH-1H on an EVI1^{Low} AML cell line (K562) and two EVI1^{High} AML cell lines (UCSD/AML1 and HNT-34) with two B-ALL cell lines (BALL1 and RAMOS) as controls. After the cells were incubated with various concentrations of CAMPATH-1H for 48 h, the cell viability was evaluated by Trypan blue staining (Figure 3a). Cell growth was inhibited in the three AML cell lines with EVI1^{High} expression in a dose-dependent manner, and 51.5–78.9% of cells remained viable at 10 μg/ml CAMPATH-1H. In contrast, over 90% of B-ALL cells were viable at this drug concentration. In the next experiment, primary AML cells from a patient with EVI1^{Low} expression (PT1) and from three patients with EVI1^{High} expression (PT8, PT9 and PT11) were used to test the direct cytotoxic effect of CAMPATH-1H. Over 90% of PT1 cells were viable at all drug concentrations; however, only 52.5–57.5% of EVI1^{High} AML cells from patients (PT8, PT9 and PT11) survived the maximal dose of 100 μg/ml, suggesting that CAMPATH-1H directly suppressed the survival of EVI1^{High} AML cells.

To confirm whether the cytotoxic effect of CAMPATH-1H is dependent on apoptotic cell death, we treated two EVI1^{High} AML cell lines (UCSD/AML1 and HNT-34) and primary EVI1^{High} AML cells (PT8) with 10 μg/ml of CAMPATH-1H for 4 days and determined the cell viability and apoptosis. In all of the EVI1^{High} AML cells, the growth rate of CAMPATH-1H-treated cells was slower than that of control immunoglobulin G (IgG)-treated cells (Figures 3b, d and f) and 15.5–40.1% of EVI1^{High} AML cells underwent apoptosis 2 days after treatment (Figures 3c, d and f). Moreover, the amount of cleaved caspase-3 (18 kDa) was increased in the EVI1^{High} leukemic cells after 2 days of CAMPATH-1H treatment (Figure 3h). Thus, our results indicate that CAMPATH-1H effectively induces apoptosis in EVI1^{High} AML cells.

CAMPATH-1H-mediated CDC and ADCC against EVI1^{High} AML cells

Because CAMPATH-1H exerts its antitumor effects on lymphocytes or lymphoid leukemia cells through immunological mechanisms, such as CDC and/or ADCC, by virtue of its

Figure 3 Induction of direct cytotoxicity against EVI1^{High} AML cells by CAMPATH-1H treatment. (**a**) Viable cells after treatment with the indicated concentration of CAMPATH-1H for 48 h were examined using Trypan blue dye exclusion and are shown as the percentages of the values obtained from the untreated parental cells. The left panel shows the percent viability of cell lines with EVI1^{Low} expression (K562, RAMOS and BALL1; dot lines with open marks) and with EVI1^{High} expression (UCSD/AML1 and HNT34; solid lines with closed marks). The right panel shows the percent viability of primary AML cells with EVI1^{Low} expression (PT1; dot lines with open marks) and with EVI1^{High} expression (PT8, PT9 and PT11; solid lines with closed marks). The experiments were performed in triplicate and repeated independently at least three times. (**b**, **d**, **f**) Viable cell numbers of EVI1^{High} AML cells (UCSD/AML1, HNT-34 and PT8) were shown at the indicated time points after treatment with 10 μg/ml of CAMPATH-1H or with control IgG. Student's *t*-test ($P<0.05$) was used for the statistical analysis between the control IgG- and CAMPATH-1H-treated AML cells. (**c**, **e**, **g**) CAMPATH-1H treatment induces the apoptosis of EVI1^{High} AML cells. Following treatment with CAMPATH-1H for 48 h, cells were labeled with Annexin-V and propidium iodide, and the percent of apoptotic cells was determined using flow cytometry. The experiments were performed in triplicate and repeated independently at least three times. (**h**) Identification of cleaved caspase-3 after the treatment with CAMPATH-1H against EVI1^{High} AML. EVI1^{High} AML cell lines (UCSD/AML1 and HNT-34) were treated with CAMPATH-1H (10 μg/ml) for 48 h, and western blot analyses were performed by anti-caspase-3 antibody. Asterisks indicate nonspecific bands.

IgG Fc region, we initially investigated the CDC activity of CAMPATH-1H on EVI1^{High} AML cell lines (UCSD/AML1 and HNT-34) along with EVI1^{Low} AML (K562) and B-ALL cell lines (BALL1 and RAMOS) as controls. CAMPATH-1H treatment induced a slight increase in cell death in the two B-ALL and two EVI1^{High} AML cell lines, although it had no effect on the EVI1^{Low} K562 cell line (Figure 4a, left panel). Next, primary AML cells from a patient with EVI1^{Low} (PT1) and from three patients with EVI1^{High} expression (PT8, PT9 and PT11) were used to test the effect of CAMPATH-1H on CDC. Only a low level of cell death was observed in the PT1 and PT8 cells, but a moderate CDC effect was observed using the PT-9 and PT11 cells (Figure 4a, right panel). Thus, CAMPATH-1H does not appear to have a significant CDC effect on EVI1^{High} AML cells.

Next, the ADCC activity of CAMPATH-1H was examined against the same cell lines and primary AML cells as those in the CDC. In the two B-ALL and two EVI1^{High} leukemia cell lines, CAMPATH-1H significantly increased the percentages of cell death in a dose-dependent manner, whereas EVI1^{Low} K562 cells showed almost no response (Figure 4b, left panel). Treatment

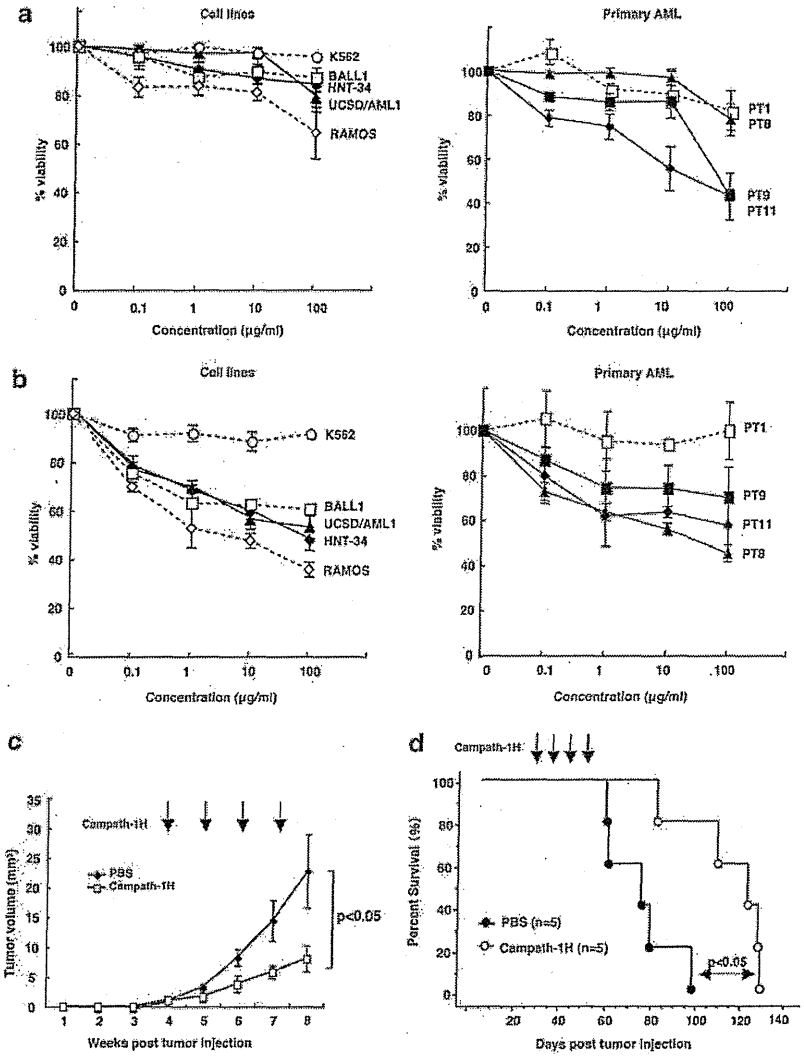

Figure 4 The induction of CDC and ADCC activities by the treatment of CAMPATH-1H and *in vivo* antitumor activity against EVI1^{High} AML cells in mouse xenograft models. (**a**) CAMPATH-1H-mediated CDC activity in various leukemia cells. The left panel shows the percent viability of cell lines with EVI1^{Low} expression (K562, RAMOS and BALL1; dot lines with open marks) and cell lines with EVI1^{High} expression (UCSD/AML1 and HNT34; solid lines with closed marks). The right panel shows the percent viability of primary AML cells with EVI1^{Low} expression (PT1; dot lines with open marks) and AML cells with EVI1^{High} expression (PT8, PT9 and PT11; solid lines with closed marks). After the cells were incubated with human serum complement and CAMPATH-1H at concentrations from 0.1 to 100 μg/ml, the extent of cell lysis was measured with an LDH-releasing assay and is shown as the percentage of the value obtained from the untreated parental cells. The experiments were repeated independently at least three times. (**b**) CAMPATH-1H-mediated ADCC activity in various leukemia cells. ADCC assays were performed with the same series of cells used in (**a**). After incubation of the cells with PB mononuclear cells from a normal donor and 0.1–100 μg/ml of CAMPATH-1H, ADCC activity was measured by LDH release. The results are the mean and standard deviations for each sample, which was independently repeated in triplicate. (**c**) CAMPATH-1H reduces tumor growth in NOG mice xenografted with EVI1^{High} AML cells. CAMPATH-1H was administered at 4 mg/kg intravenously weekly for 4 weeks. Tumor growth was assessed by measuring the volume of each tumor at weekly intervals. Each group contained five mice. The graphs depict the average tumor volume for the PBS control group and the CAMPATH-1H-treated group ± standard error (**d**) Kaplan–Meier survival plot of UCSD/AML1-bearing NOG mice. CAMPATH-1H was administered at 4 mg/kg intravenously weekly for 4 weeks. Kaplan–Meier survival curves are shown for PBS- and CAMPATH-1H-treated groups ($n=5$ per group).